

CRANIAL NEURAL CREST CELL MIGRATION IN THE AVIAN EMBRYO AND  
THE ROLES OF EPH-A4 AND EPHRIN-A5

Thesis by  
Carole Chih-Chen Lu

In Partial Fulfillment of the Requirements  
for the degree of  
Doctor of Philosophy

California Institute Of Technology

Pasadena, California

2007

(Defended September 21, 2006)

© 2007

Carole Chih-Chen Lu

All Rights Reserved

## ACKNOWLEDGEMENTS

My relationship with developmental biology began in 1998, when I took my first developmental biology class. To me, it was love at first sight. Since arriving at graduate school, the path has been mostly uphill, and there are many people who have supported, motivated, and kept me on the path.

I thank my advisor and mentor, Scott E. Fraser, for his guidance and support all these years. Scott provides a unique research environment where graduate students are given freedom to pursue scientific questions. He is also incredibly supportive and has (what must be) an infinite supply of optimistic advice.

I thank the members of my committee, Marianne Bronner-Fraser, Paul Sternberg, and David Chan for scientific guidance and expertise.

The Fraser lab is intimate because it is filled with friendly and helpful colleagues. I thank Paul Kulesa, who thoroughly and patiently showed me the ropes and provided me with a solid foundation. I thank Sean Megason, Helen McBride, Elaine Bearer, and Andrew Ewald for invaluable scientific discussions and knowledge. I thank Michael Liebling for expertise with image analysis software, David Koos for advice in molecular biology and histology, Tatyana Demyanenko for advice in histology, and Aura Keeter for invaluable technical support. I thank Mary Flowers for being our lab mom, Gary Belford and Sonia Collazo for their skilled computer technical support. I thank Chris Waters and Dan Darcy for maintaining our confocal systems. I also thank Julien Vermot, Le Trinh, Robia Pautler, Christie Canaria, Max Ezin, Mat Barnet, Larry Wade, Magdalena Bak-Maier, David Wu, Rusty Lansford, Mary Dickinson, Liz Jones, and Arian Forouhar for being awesome lab mates.

I thank Marianne Bronner-Fraser for a wonderful teaching assistant experience and scientific discussions. The Bronner-Fraser lab next door graciously helps us with reagents and discussions. Specifically I thank Meghan Adams, Sujata Bhattacharyya, Vivian Lee, Martin Basch, Martin Garcia-Castro, Tatjana Sauka-Spengler, Ed Coles, Lisa Taneyhill, and Meyer Barembaum.

My fellow classmates were invaluable during graduate school. Specifically, I thank Gloria Choi, Pei-Yun Lee, and Magdalena Bak-Maier for the fun that we had when we studied for and passed our quals. Toby Rosen, Karli Watson, Xavier Ambroggio, and Johannes Graumann are great fun. I thank Sean Megason and Bernadine Tsung-Megason for adventures outside of lab. I thank Stuart Freed for not throwing out my pots at the pottery studio and for years of therapeutic pottery.

I thank my dear sisters, Connie Lu and Cathy Lu, for providing me with many photographic opportunities and material for funny stories. I thank Attila Kovacs for feeding Connie. My parents, Kuen and Dong-Chih Lu, have consistently kept me on the path to graduation.

Lastly, I thank Alok J. Saldanha, my husband, for his love, brilliance, and enthusiasm. Alok is passionate about the world and is the best life partner that I could have ever hoped for.

In memory of Eric Tse and Ben Edelson.

In memory of Molly.

## ABSTRACT

The neural crest is a transient population of cells that migrate away from the dorsal neural tube in the vertebrate embryo. As the developing hindbrain constricts into rhombomeres, cranial neural crest cells migrate in three discrete streams adjacent to even-numbered rhombomeres, rhombomere 2 (r2), r4, and r6.

To test the role of intrinsic versus extrinsic cues in influencing an individual cell's trajectory, we implanted physical barriers in the chick mesoderm, distal to emerging neural crest cells (NCCs). We analyzed spatio-temporal dynamics as NCCs encountered and responded to the barriers by using time-lapse confocal microscopy and cell tracking analysis. The majority of NCCs were able to overcome physical barriers. Even though the lead cells become temporarily blocked by a barrier, follower cells find a novel pathway around a barrier and become de novo leaders of a new stream. Quantitative analyses of cell trajectories find cells that encounter an r3 barrier migrate significantly faster but less directly than cells that encounter an r4 barrier, which migrate normally. NCCs can also migrate into normally repulsive territory as they reroute. These results suggest that cranial neural crest cell trajectories are not intrinsically determined. NCCs can respond to minor alterations in the environment to retarget a peripheral destination. Both intrinsic and extrinsic cues are important in patterning.

We then tested the role of Eph/ephrin signaling on cranial neural crest migration by ectopically expressing full-length ephrin-A5 ligand; a truncated,

constitutively active EphA4 receptor; and a truncated, kinase-dead EphA4 receptor within migratory neural crest cells. Ectopic expression of ephrin-A5 specifically causes the r6 subpopulation of neural crest cells to have truncated migration but does not affect directionality, suggesting that the r6 neural crest cells properly follow guidance cues. Our results support a role for ephrin-A5 in regulating the extent of migration.

Ectopic expression of constitutively active, truncated EphA4 causes NCCs to migrate aberrantly around the otic vesicle. Pathfinding errors are accompanied by changes in migratory behavior, with the NCCs migrating faster but with less directionality. Expression of a truncated, kinase-dead version of EphA4 also leads to pathfinding errors. Our results suggest Eph activity is involved in guidance and extent of migration.

## TABLE OF CONTENTS

ACKNOWLEDGEMENTS .....	iii
ABSTRACT.....	v
TABLE OF CONTENTS .....	vii
LIST OF FIGURES.....	ix
LIST OF TABLES .....	x
CHAPTER 1: Introduction .....	1
<i>Introduction</i> .....	1
<i>Avian embryo</i> .....	1
<i>Cranial neural crest cells: what are they and why are they important?</i> .....	2
<i>Stereotypical pattern of migration</i> .....	4
<i>Possible intrinsic and extrinsic mechanisms</i> .....	5
<i>Goal of this thesis</i> .....	8
<i>References</i> .....	14
CHAPTER 2: Time-lapse analysis reveals a series of events by which cranial neural crest cells reroute around physical barriers .....	20
<i>Abstract</i> .....	20
<i>Introduction</i> .....	22
<i>Materials and Methods</i> .....	27
<i>Results</i> .....	31
<i>Discussion</i> .....	36
<i>Acknowledgements</i> .....	41
<i>References</i> .....	41
<i>Figures</i> .....	45
CHAPTER 3: Time-lapse analysis of perturbations of ephrin-A5 and EphA4 during cranial neural crest migration in the avian embryo .....	55
<i>Abstract</i> .....	55
<i>Introduction</i> .....	57
<i>Materials and Methods</i> .....	61
<i>Results</i> .....	65

<i>Discussion</i> .....	73
<i>Acknowledgements</i> .....	79
<i>References</i> .....	79
<i>Figures</i> .....	88
CHAPTER 4: Summary and Future Directions.....	108
<i>Summary</i> .....	108
<i>Future Directions</i> .....	111
<i>References</i> .....	114

## LIST OF FIGURES

<i>Figure 1.0: Stereotypical pattern of migration</i> .....	11
<i>Figure 2.1: Foil barriers are ineffective at blocking cranial neural crest</i> .....	45
<i>Figure 2.2: Leaders and followers change when a population of neural crest cells encounters a barrier</i> .....	47
<i>Figure 2.3: Neural crest cells that are blocked behind the barrier tend to migrate faster than cells that go around the barrier</i> .....	49
<i>Figure 2.4: Neural crest cells are able to migrate into the r3 repulsive zone by migrating on top of each other</i> .....	51
<i>Figure 3.1: Differential expression of EphA4 and ephrin-A5 within the cranial region of an HH12 embryo</i> .....	88
<i>Figure 3.2: Ectopic ephrin-A5 expression leads to fewer NCCs in BA3 initially</i> .....	90
<i>Figure 3.3: Neural crest cells ectopically expressing ephrin-A5 do not migrate to BA3</i> .....	92
<i>Figure 3.4: Ephrin-A5+ r6 NCCs do not migrate to BA4</i> .....	94
<i>Figure 3.5: EphA4(int) and EphA4(kd) causes mismigration along the otic vesicle</i> .....	95
<i>Figure 3.6: Cell morphology, temporal distribution, and cell-tracking</i> .....	96
<i>Figure 3.7: Eph/ephrin concentration and migration</i> .....	98
<i>Figure 3.8: Ectopic ephrin-A5 and EphA4 activity</i> .....	100
<i>Figure 3.9: Summary of ephrin-A5 and EphA4 perturbations</i> .....	102
<i>Supplementary materials: cell death and cell proliferation</i> .....	106
<i>Figure 4.0: Distinct mechanisms guide neural crest migration at r4 and r6</i> .....	116

## LIST OF TABLES

<i>Table 2.1: Mean velocity and directionality for barriers at r3 and r4</i> .....	53
<i>Table 3.1: Cell tracking analysis: cranial neural crest cells</i> .....	103
<i>Table 3.2: Cell tracking analysis: r6 subpopulation of cranial neural crest cells</i> .....	104
<i>Table 3.3: Rates of cell proliferation and death</i> .....	105

## KEYWORDS

avian embryo

cell migration

cell-tracking

confocal microscopy

cranial neural crest

electroporation

EphA4

ephrin-A5

foil barrier

particle-tracking

time-lapse imaging

whole-embryo explant culture

## CHAPTER 1: Introduction

### ***Introduction***

The process by which we develop out of a single fertilized egg is wonderfully complex. In theory, it is easy to understand— one cell divides into two daughter cells that too go on to divide until there is a population of cells that makes up an entire organism. How do we end up being a complex organism rather than a clump of cells? How do cells become patterned and coordinated into structures? The question of pattern formation is a global one. Cell division is but one aspect of development. From the cell's point of view, there are many different choices along the way. Not only can they divide, but also they can die, differentiate, migrate, respond to cues in the environment, secrete cues into the environment, or any combination of the above. All these actions by individual cells need to occur in an orchestrated fashion such that at the end, there is a complete and functional multi-cellular organism. During my tenure as a graduate student, I chose the migration of cranial neural crest cells within the avian embryo as the system in which to address how migration is involved in pattern formation.

### ***Avian embryo***

The avian embryo has been a classic system for embryological studies since Aristotle (Aristotle, 350 B.C.E) for a number of reasons. Fresh, fertilized eggs are easy to obtain, available year round, relatively cheap, develop externally, and are easy to handle within a laboratory setting. The Hamburger

and Hamilton staging series (1951) allows one to conveniently set eggs for a certain amount of time to obtain embryos at the desired developmental stage. A good anatomical understanding of the embryo is also available (Bellairs and Osmond, 2005). The accessibility and size of the embryo allows many types of microsurgical techniques such as ablation and grafting. Beside these more classic, embryological types of studies, new techniques have allowed us to take advantage of recent advances in molecular and cell biology. We can functionally test the roles of certain proteins or genes by implantation of protein-soaked beads; electroporation of DNA constructs, mRNA, or morpholinos; and viral transfection (Bronner-Fraser, 1996; Itasaki et al., 1999; Momose et al., 1999; Okada et al., 1999; Swartz et al., 2001; Thakur et al., 2001). The chick genome has been sequenced and allows researchers to take advantage of newly available genomic resources (reviewed in Antin and Konieczka, 2005). The chick genome offers an interesting evolutionary perspective since it is positioned between lower vertebrates, such as fish, and higher vertebrates, such as humans. Lastly, since the avian embryo is a vertebrate embryo, many of the things we learn will be relevant to understanding human development.

***Cranial neural crest cells: what are they and why are they important?***

The neural crest is a transient population of multipotent embryological cells found in vertebrate embryos. Found along most of the anteroposterior axis of the embryo, the neural crest cells are specified between the neuroectoderm and prospective ectoderm. As the neural plate folds, invaginates, and fuses to

form the neural tube, the neural crest cells delaminate from their neighbors at the dorsal part of the neural tube. The neural crest cells then migrate away from the neural tube along a number of different pathways to give rise to a variety of cells, including glia, neurons, cartilage, and bone (Douarin et al., 1994).

Cranial neural crest cells are the subpopulation of neural crest cells that arise in the head. As cranial neural crest cells migrate into the periphery, they are an important source of proliferative, mesenchymal cells and contribute to all of the skeletal and connective tissues (except for tooth enamel). Defects in cranial neural crest development can lead to congenital craniofacial abnormalities (Sadler, 2000). Some abnormalities, such as craniosynostosis, or premature fusion of skull plates, are caused by defects in differentiation. Others, such as Treacher Collins and Pierre Robin syndromes, are thought to arise from defects in migration (reviewed in Farlie et al., 2004). Understanding the biology of cranial neural crest cells is crucial to understanding craniofacial development and important in figuring out how craniofacial defects occur.

The ability to migrate is fundamental to neural crest cell identity. It is very difficult to discern a neural crest cell from neighboring neural tube cells until the neural crest cell begins to undergo an epithelial to mesenchymal transition and migrate away from the neural tube. In fact, neural crest cells and neural tube cells can even share the same progenitor (Bronner-Fraser and Fraser, 1988). Along the midbrain (Figure 1.0A, MB), the cranial neural crest cells migrate as a wave of cells that fills in the surrounding mesenchyme in a U-shaped domain (Kulesa and Fraser, 1998a). In the hindbrain (Figure 1.0A, HB), the cranial neural

crest cells migrate as three discrete streams (Figure 1.0C, green arrows) deployed from even-numbered rhombomeres, i.e., rhombomeres 2 (r2), r4, and r6 (Birgbauer et al., 1995; Kulesa and Fraser, 1998a; Sechrist et al., 1993) that fill in branchial arches 1 (BA1), BA2, and BA3, which are lateral epidermal pouches. Neural crest cells from odd-numbered rhombomeres migrate anteriorly or posteriorly in order to join neural crest cells from even-numbered rhombomeres (Figure 1.0 C red arrows). Therefore, the stream from rhombomere 4 (r4) consists of neural crest cells from r3, r4, and r5, and migrates to BA2.

### ***Stereotypical pattern of migration***

The pattern of three discrete streams of migratory neural crest cells from the hindbrain (Figure 1.0A, B) is believed to serve an important function in preserving the segmentation that occurs in the head. The hindbrain first forms as a tube that physically constricts into segments called rhombomeres (Hunt et al., 1991a; Kulesa and Fraser, 1998b; Vaage, 1969). Cells within each rhombomere tend to stay segregated from neighboring rhombomere (Fraser et al., 1990). Each rhombomere expresses its own set of segmentation genes, such as members of the Hox family, Eph/ephrins, and transcription factor Krox-20. Migratory neural crest cells often express the same segmentation genes as their rhombomere of origin. One model is that the neural crest cells carry this segmental identity to pattern the unsegmented, peripheral mesenchyme (Hunt et al., 1991b). The anteroposterior organization of the neural crest is preserved in

the cranial skeletomuscular structures that they form (Kontges and Lumsden, 1996). The migration of the cranial neural crest cells within discrete streams is thought to play an important role in maintaining this segmental patterning. There are several different models for initiating and maintaining migration in three different streams.

### ***Possible intrinsic and extrinsic mechanisms***

There have been a number of different mechanisms postulated to shape the migratory cranial neural crest cell populations into three discrete streams from the hindbrain. In general, they can be categorized as intrinsic or extrinsic mechanisms as described below and diagramed in Figure 1.1. Intrinsic mechanisms, loosely defined as those that act within the neural crest cells themselves, include localized cell death, population pressure, and differential affinity. These mechanisms suggest that the discrete pattern of migration is set up within the neural tube, and the neural crest cells follow this initial pattern as they migrate away from the neural tube. Extrinsic mechanisms suggest that the neural crest cells follow cues found in the environment external to the neural tube, and adjust migration accordingly. Guidance cues within the environment, such as strategically placed attractive or repulsive cues, are believed to play a key role in shaping the migration pathway by either attracting or repulsing migratory neural crest cells.

One line of thought is that the hindbrain neural crest cells are organized into discrete subpopulations before they exit the neural tube. One possible

mechanism for shaping discrete streams is localized cell death within r3 and r5 (Figure 1.1A, red X). Within the neuroepithelium, the expression of *Msx-2* precedes localized domains of apoptosis (Ellies et al., 2000; Graham et al., 1993). However, other studies in chick, mouse, and zebrafish have found that r3 and r5 are in fact capable of generating neural crest cells, which actively migrate along diagonal trajectories in order to join streams from even-numbered rhombomeres (Birgbauer et al., 1995; Kulesa and Fraser, 1998a; Schilling and Kimmel, 1994; Sechrist et al., 1993; Trainor and Krumlauf, 2000b). Another variation is that of exit points (Figure 1.1B), where the neural crest cells from odd-numbered rhombomeres are only able to exit the neural tube at the boundary between even/odd rhombomeres (Figure 1.1B, small green arrows), which would also lead to a discrete migratory pattern (Birgbauer et al., 1995; Lumsden et al., 1991; Niederlander and Lumsden, 1996).

Early segregation of the neural crest cells could be maintained by population pressure (reviewed in Le Douarin and Kalcheim, 1999; Newgreen et al., 1979) whereby follower cells push upon leader cells and migrate along signals generated by leader cells (Figure 1.1D). The r4 stream is shaped such that the front of stream is fan-shaped whereas the rest of the stream follows behind in a very tight and narrow path from the neural tube. Cells at the front of the migration stream migrate in more directed paths than their followers (Kulesa and Fraser, 1998a), which also supports the idea that, within any given stream, there is a difference in how the neural crest cells at the front and back of the stream perceive guidance cues.

Differential affinity generally explains how neural crest cells from one rhombomere will tend to migrate together, in one stream, rather than mix with cells from other rhombomeres in neighboring streams (Figure 1.1C). Cells from even- and odd-numbered rhombomeres tend to stay segregated from each other (Fraser et al., 1990; Lumsden and Guthrie, 1991), though this affinity is lost at the end of the migration process and the neural crest cells reach the branchial arches (Hunt and Hunt, 2003). In *Xenopus*, the differential expression of surface ligand ephrin-B2 with receptors EphA4/EphB2 or proper levels of EphA activity is thought to be the molecular cues that keep the third arch neural crest cells from migrating into the second or fourth arch (Helbling et al., 1998; Smith et al., 1997). Questions remain as to whether the Eph/ephrin signaling pathway is also involved in the migration of avian cranial neural crest cells.

Besides these mechanisms, which rely on properties intrinsic to the neural crest cells, there is also mounting evidence supporting the role of extrinsic cues. Cranial neural crest cell migration is a highly regulative process, and migratory pathways are often somewhat plastic. Transplanted or rotated neural crest cells will migrate and change Hox gene expression according to their new location (Sechrist et al., 1994; Trainor and Krumlauf, 2000a; Trainor et al., 2002). In addition, neural crest cells have the ability to fill in for ablated neighbors by modifying their migratory pathways (Kulesa et al., 2000) and to generate normal looking structures (Saldivar et al., 1997). All of this points to an inherent ability in neural crest cells to regulate their migratory pathway according to environmental cues.

Some possible environmental cues include repulsive cues within the r3 and r5 paraxial mesoderm, which are important in shaping the r4 stream (Figure 1.1E). Neural crest cells transplanted to the paraxial mesoderm adjacent to r3 or r5 divert, suggesting that there are negative guidance cues from exclusion zones anterior and posterior of the r4 stream (Farlie et al., 1999). R3 and the r3 surface ectoderm are required for repulsion of the r4 neural crest cells (Golding et al., 2002; Golding et al., 2000). Likewise, the r5 surface ectoderm is required to maintain the crest-free zone in the r5 paraxial mesoderm (Golding et al., 2004). Molecularly, ErbB4 is thought to maintain the repulsion zone adjacent to r3, although other cues are likely to be involved as well (Golding et al., 2004). How exactly these environmental guidance cues mesh with intrinsic properties of the neural crest cells is still under investigation.

### ***Goal of this thesis***

This thesis seeks to test some of the above mechanisms and understand how migratory behavior fits into the picture, in the context of cranial neural crest cell migration. To do this, we take a two-pronged approach: physical and molecular.

In Chapter 2, we first examine the extent to which the pathway of migration is stereotypical and, at the same time, test the fidelity of the neural crest cells to migrate along their normal pathways. We examine the plasticity and capacity to migrate without directly disturbing molecular cues within the neural crest cells or external environment. Specifically, we test the ability of the r4

neural crest cells to migrate around a physical barrier. Since the r4 stream migrates along a well-defined, dense pathway, our physical barrier experiments test whether neural crest cells adhere to strict intrinsic directions as they migrate or whether (and how) they adjust to changes in the environment. We show that population pressure does not seem to play a major role in driving migration around the barrier, that the roles of leaders and followers are interchangeable within the neural crest cell population, and that neural crest cells have the ability to migrate along each other, even in normally repulsive territory. Barrier positions elicit differential migratory behavior and provide tantalizing clues as to how the neural crest cells might migrate depending on the availability of guidance cues. Our results highlight the ability of the neural crest cells to pathfind and forge new migratory pathways. Our first approach highlights the robustness of the migratory neural crest cells to “read” environmental cues and to pathfind around physical barriers.

In Chapter 3, we examine the molecular cues that might be involved during migration. To do this we study the effects of perturbations to the Eph/ephrin signaling pathway on the migration of cranial neural crest cells. In the avian embryo, the post-otic neural crest cells begin migration in a wave that then segregates and fills BA3 and BA4. We choose to perturb the activity of Eph/ephrin within migratory neural crest cells by the expression of full-length ephrin-A5 and two forms of EphA4— a truncated, constitutively active form of the intracellular domain of EphA4, and the kinase-dead version. Ectopic expression of ephrin-A5 leads to truncated migration of the r6 neural crest cells. The other

hindbrain neural crest cells are unaffected, in terms of both pathfinding and migratory behavior. Ectopic EphA4 activity, on the other hand, leads to aberrant migration of neural crest cells within the r4 and r6 streams along the otic vesicle. Erratic pathfinding is coupled with increased velocity and lowered directionality. Our studies with ephrin-A5 and EphA4 points to diverse functions for Eph/ephrin signaling within the neural crest cells. Ephrin-A5 is likely to be involved in the maintenance of migration, rather than in pathfinding. EphA4, on the other hand, is likely involved in pathfinding as well as regulation of how much migration takes place.

*Figure 1.0: Stereotypical pattern of migration*

(A) Neural crest cells migrate in three discrete streams from the hindbrain of an HH11 stage chick embryo where the premigratory neural crest cells have been labeled with Dil. (B) Neural tube cells and migratory neural crest cells are labeled in Dil. Three discrete streams are visible. (C) Streams of neural crest cells form adjacent to even-numbered rhombomeres (green arrows). Pathways for neural crest cells from odd-numbered rhombomeres and first few somite levels are shown in red. MB midbrain, HB hindbrain, BA1 branchial arch 1, r2 rhombomere 2. Scalebar 200  $\mu$ m.

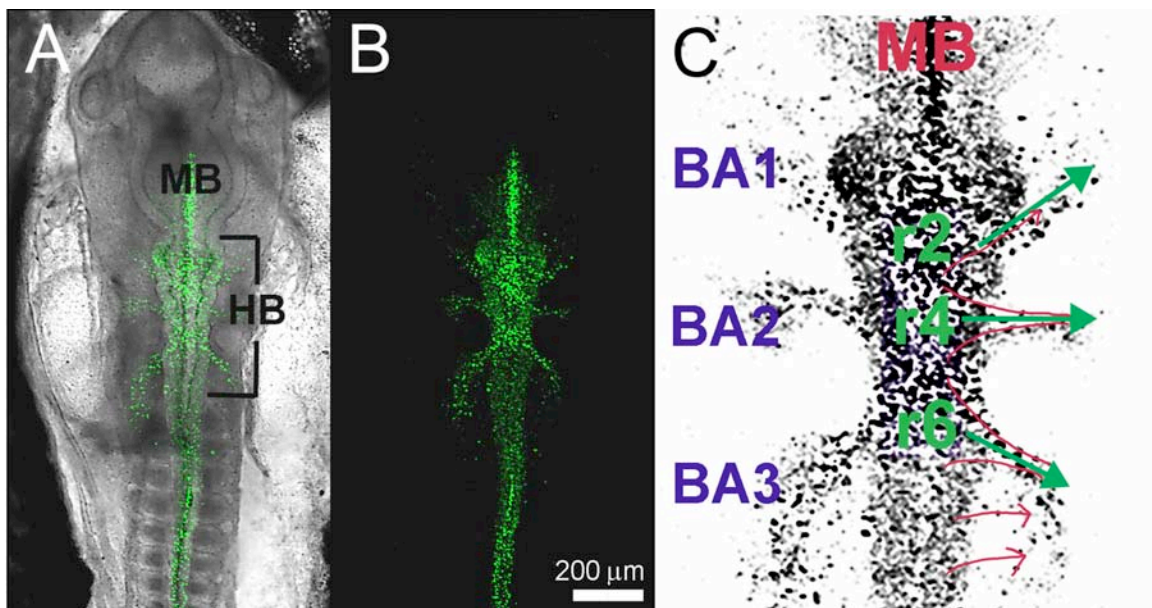
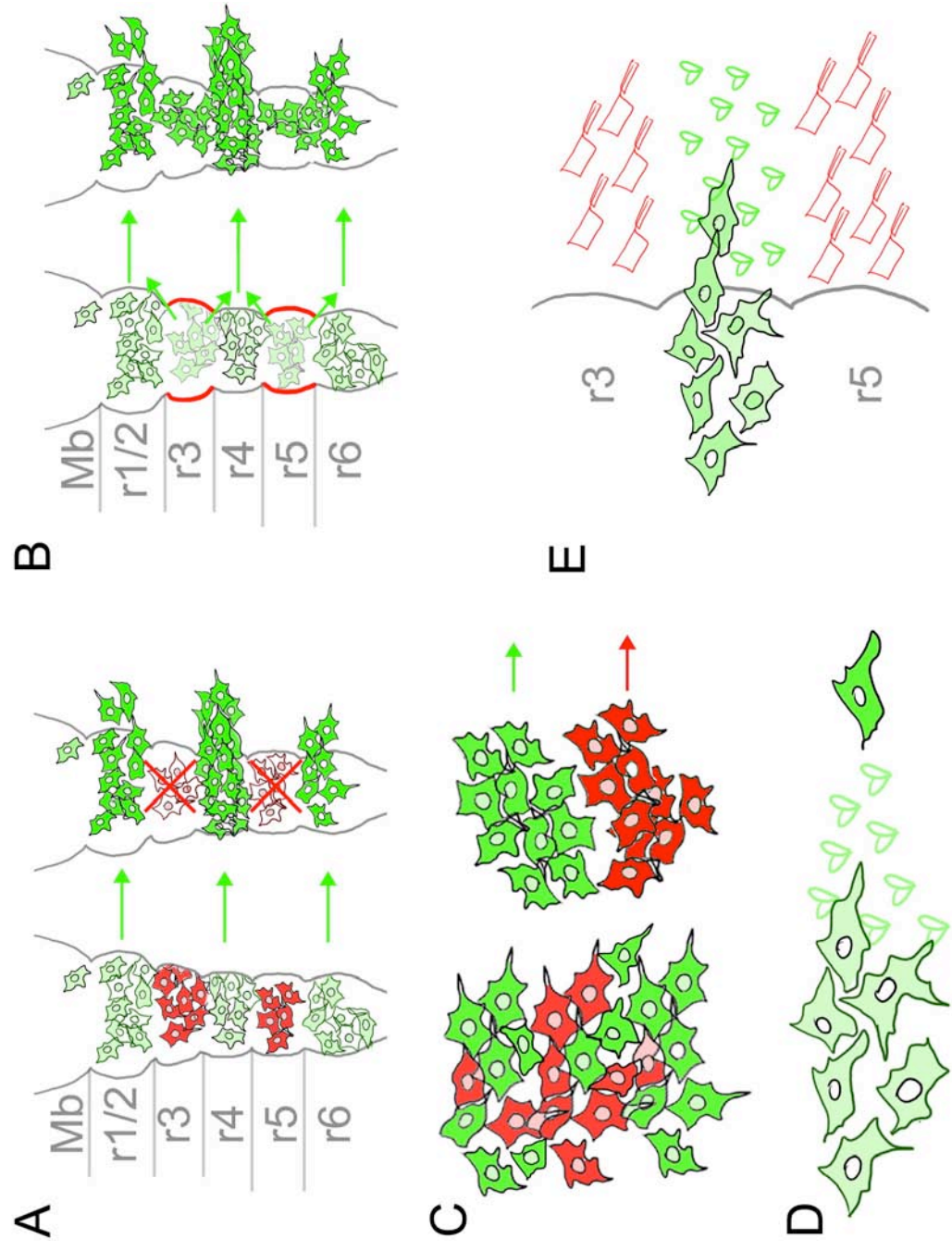


*Figure 1.1: Intrinsic and extrinsic mechanisms for guiding migration*

Both intrinsic and extrinsic mechanisms may be involved in shaping the migration of the cranial neural crest cells from the hindbrain into three streams. (A) Localized cell death at r3 and r5 (marked by “X”, red cells) removes these subpopulations of neural crest cells. Migrating neural crest cells only arise from r1/2, r4, and r6. (B) Exit points at the boundary between even- and odd-numbered rhombomeres force the neural crest cells from r3 and r5 to migrate diagonally before joining the streams from r1/2, r4 and r6. The region adjacent to r3 and r5 (red lines) does not allow the neural crest cells to cross. (C) Differential affinity can be established within the rhombomere and encourages neural crest cells to preferentially associate with “like” cells (i.e., green or red) and to migrate together. (D) One aspect of population pressure is that the follower cells (light green) will migrate towards guidance cues (green hearts) secreted by the lead cells (dark green). (E) Extrinsic guidance cues can be in the form of repulsive cues (red cleavers) and attractive cues (green hearts) that shape the pathway in which the neural crest cells can migrate.



**References**

- Antin, P. B. and Konieczka, J. H.** (2005). Genomic resources for chicken. *Dev Dyn* **232**, 877-82.
- Aristotle.** (350 B.C.E). The History of Animals.
- Bellairs, R. and Osmond, M.** (2005). Atlas of Chick Development. San Diego: Academic Press.
- Birgbauer, E., Sechrist, J., Bronner-Fraser, M. and Fraser, S.** (1995). Rhombomeric origin and rostrocaudal reassortment of neural crest cells revealed by intravital microscopy. *Development* **121**, 935-45.
- Bronner-Fraser, M.** (1996). Methods in Avian Embryology. San Diego: Academic Press.
- Bronner-Fraser, M. and Fraser, S. E.** (1988). Cell lineage analysis reveals multipotency of some avian neural crest cells. *Nature* **335**, 161-4.
- Douarin, N., Dupin, E. and Ziller, C.** (1994). Genetic and Epigenetic Control in Neural Crest Development. *Curr Opin Genet Dev.* **4**, 685-695.
- Ellies, D. L., Church, V., Francis-West, P. and Lumsden, A.** (2000). The WNT antagonist cSFRP2 modulates programmed cell death in the developing hindbrain. *Development* **127**, 5285-95.
- Farlie, P. G., McKeown, S. J., Newgreen, D. F.** (2004) The neural crest: basic biology and clinical relationships in the craniofacial and enteric nervous systems. *Birth Defects Res C Embryo Today* **72**, 173-89.
- Farlie, P. G., Kerr, R., Thomas, P., Symes, T., Minichiello, J., Hearn, C. J. and Newgreen, D.** (1999). A paraxial exclusion zone creates patterned cranial

neural crest cell outgrowth adjacent to rhombomeres 3 and 5. *Dev Biol* **213**, 70-84.

**Fraser, S., Keynes, R. and Lumsden, A.** (1990). Segmentation in the chick embryo hindbrain is defined by cell lineage restrictions. *Nature* **344**, 431-5.

**Golding, J. P., Dixon, M. and Gassmann, M.** (2002). Cues from neuroepithelium and surface ectoderm maintain neural crest-free regions within cranial mesenchyme of the developing chick. *Development* **129**, 1095-105.

**Golding, J. P., Sobieszczuk, D., Dixon, M., Coles, E., Christiansen, J., Wilkinson, D. and Gassmann, M.** (2004). Roles of ErbB4, rhombomere-specific, and rhombomere-independent cues in maintaining neural crest-free zones in the embryonic head. *Dev Biol* **266**, 361-72.

**Golding, J. P., Trainor, P., Krumlauf, R. and Gassmann, M.** (2000). Defects in pathfinding by cranial neural crest cells in mice lacking the neuregulin receptor ErbB4. *Nat Cell Biol* **2**, 103-9.

**Graham, A., Heyman, I. and Lumsden, A.** (1993). Even-numbered rhombomeres control the apoptotic elimination of neural crest cells from odd-numbered rhombomeres in the chick hindbrain. *Development* **119**, 233-45.

**Helbling, P. M., Tran, C. T. and Brandli, A. W.** (1998). Requirement for EphA receptor signaling in the segregation of *Xenopus* third and fourth arch neural crest cells. *Mech Dev* **78**, 63-79.

**Hunt, P., Whiting, J., Muchamore, I., Marshall, H. and Krumlauf, R.** (1991a). Homeobox genes and models for patterning the hindbrain and branchial arches. *Dev Suppl* **1**, 187-96.

**Hunt, P., Whiting, J., Nonchev, S., Sham, M. H., Marshall, H., Graham, A., Cook, M., Allemann, R., Rigby, P. W., Gulisano, M. et al.** (1991b). The branchial Hox code and its implications for gene regulation, patterning of the nervous system and head evolution. *Development Suppl 2*, 63-77.

**Hunt, R. and Hunt, P. N.** (2003). The role of cell mixing in branchial arch development. *Mech Dev 120*, 769-90.

**Itasaki, N., Bel-Vialar, S. and Krumlauf, R.** (1999). 'Shocking' developments in chick embryology: electroporation and in ovo gene expression. *Nat Cell Biol 1*, E203 - E207.

**Kontges, G. and Lumsden, A.** (1996). Rhombencephalic neural crest segmentation is preserved throughout craniofacial ontogeny. *Development 122*, 3229-3242.

**Kulesa, P., Bronner-Fraser, M. and Fraser, S.** (2000). In ovo time-lapse analysis after dorsal neural tube ablation shows rerouting of chick hindbrain neural crest. *Development 127*, 2843-52.

**Kulesa, P. M. and Fraser, S. E.** (1998a). Neural crest cell dynamics revealed by time-lapse video microscopy of whole embryo chick explant cultures. *Dev Biol 204*, 327-44.

**Kulesa, P. M. and Fraser, S. E.** (1998b). Segmentation of the vertebrate hindbrain: a time-lapse analysis. *Int J Dev Biol 42*, 385-92.

**Le Douarin, N. and Kalcheim, C.** (1999). *The Neural Crest*, 2nd ed. Cambridge: Cambridge University Press.

- Lumsden, A. and Guthrie, S.** (1991). Alternating patterns of cell surface properties and neural crest cell migration during segmentation of the chick hindbrain. *Development Suppl* **2**, 9-15.
- Lumsden, A., Sprawson, N. and Graham, A.** (1991). Segmental origin and migration of neural crest cells in the hindbrain region of the chick embryo. *Development* **113**, 1281-91.
- Momose, T., Tonegawa, A., Takeuchi, J., Ogawa, H., Umesono, K. and Yasuda, K.** (1999). Efficient targeting of gene expression in chick embryos by microelectroporation. *Dev Growth Differ* **41**, 335-44.
- Newgreen, D. F., Ritterman, M. and Peters, E. A.** (1979). Morphology and behaviour of neural crest cells of chick embryo in vitro. *Cell Tissue Res* **203**, 115-40.
- Niederlander, C. and Lumsden, A.** (1996). Late emigrating neural crest cells migrate specifically to the exit points of cranial branchiomotor nerves. *Development* **122**, 2367-74.
- Okada, A., Lansford, R., Weimann, J. M., Fraser, S. E. and McConnell, S. K.** (1999). Imaging cells in the developing nervous system with retrovirus expressing modified green fluorescent protein. *Exp Neurol* **156**, 394-406.
- Sadler, T. W.** (2000). *Langman's Medical Embryology*: Lippincott Williams & Wilkin.
- Saldivar, J. R., Sechrist, J. W., Krull, C. E., Ruffins, S. and Bronner-Fraser, M.** (1997). Dorsal hindbrain ablation results in rerouting of neural crest migration

and changes in gene expression, but normal hyoid development. *Development* **124**, 2729-39.

**Schilling, T. F. and Kimmel, C. B.** (1994). Segment and cell type lineage restrictions during pharyngeal arch development in the zebrafish embryo. *Development* **120**, 483-94.

**Sechrist, J., Scherson, T. and Bronner-Fraser, M.** (1994). Rhombomere rotation reveals that multiple mechanisms contribute to the segmental pattern of hindbrain neural crest migration. *Development* **120**, 1777-90.

**Sechrist, J., Serbedzija, G. N., Scherson, T., Fraser, S. E. and Bronner-Fraser, M.** (1993). Segmental migration of the hindbrain neural crest does not arise from its segmental generation. *Development* **118**, 691-703.

**Smith, A., Robinson, V., Patel, K. and Wilkinson, D. G.** (1997). The EphA4 and EphB1 receptor tyrosine kinases and ephrin-B2 ligand regulate targeted migration of branchial neural crest cells. *Curr Biol* **7**, 561-70.

**Swartz, M., Eberhart, J., Mastick, G. S. and Krull, C. E.** (2001). Sparking new frontiers: using in vivo electroporation for genetic manipulations. *Dev Biol* **233**, 13-21.

**Thakur, A., Lansford, R., Thakur, V., Narone, J. N., Atkinson, J. B., Buchmiller-Crair, T. and Fraser, S. E.** (2001). Gene transfer to the embryo: strategies for the delivery and expression of proteins at 48 to 56 hours postfertilization. *J Pediatr Surg* **36**, 1304-7.

**Trainor, P. A.** (2005). Specification of neural crest cell formation and migration in mouse embryos. *Semin Cell Dev Biol* **16**, 683-93.

**Trainor, P. and Krumlauf, R.** (2000a). Plasticity in mouse neural crest cells reveals a new patterning role for cranial mesoderm. *Nature Cell Biology* **2**, 96-102.

**Trainor, P. A. and Krumlauf, R.** (2000b). Patterning the cranial neural crest: hindbrain segmentation and Hox gene plasticity. *Nat Rev Neurosci* **1**, 116-24.

**Trainor, P. A., Sobieszczuk, D., Wilkinson, D. and Krumlauf, R.** (2002). Signalling between the hindbrain and paraxial tissues dictates neural crest migration pathways. *Development* **129**, 433-42.

**Vaage, S.** (1969). The segmentation of the primitive neural tube in chick embryos (*Gallus domesticus*). A morphological, histochemical and autoradiographical investigation. *Ergeb Anat Entwicklungsgesch* **41**, 3-87.

## **CHAPTER 2: Time-lapse analysis reveals a series of events by which cranial neural crest cells reroute around physical barriers**

This work was done in collaboration with Paul M. Kulesa and published in *Brain Behav. Evol.* 2005; 66:255-65 by S. Karger, AG. Basel, Switzerland.

### ***Abstract***

Segmentation is crucial to the development of the vertebrate body plan. Underlying segmentation in the head is further revealed when cranial neural crest cells emerge from even-numbered rhombomeres in the hindbrain to form three stereotypical migratory streams that lead to the peripheral branchial arches. To test the role of intrinsic versus extrinsic cues in influencing an individual cell's trajectory, we implanted physical barriers in the chick mesoderm, distal to emerging neural crest cell stream fronts. We analyzed the spatio-temporal dynamics as individual neural crest cells encountered and responded to the barriers, using time-lapse confocal imaging. We find the majority of neural crest cells reach the branchial arch destinations, following a repeatable series of events by which the cells overcome the barriers. Even though the lead cells become temporarily blocked by a barrier, cells that follow from behind find a novel pathway around a barrier and become *de novo* leaders of a new stream. Surprisingly, quantitative analyses of cell trajectories show that cells that encounter an r3 barrier migrate significantly faster but less directly than cells that encounter an r4 barrier, which migrate normally. Interestingly, we also find that

cells temporarily blocked by the barrier migrate slightly faster and change direction more often. In addition, we show that cells can be forced to migrate into normally repulsive territory. These results suggest that cranial neural crest cell trajectories are not intrinsically determined, that cells can respond to minor alterations in the environment and retarget a peripheral destination, and that both intrinsic and extrinsic cues are important in patterning.

## ***Introduction***

The vertebrate embryo is segmented along the anteroposterior and dorsoventral axes into different structures and domains early during development (for review, see Lumsden and Krumlauf, 1996). In the head, the hindbrain is segmented into contiguous units called rhombomeres (Vaage, 1969), which are particularly important in patterning neural crest cell migratory pathways. Soon after rhombomere boundaries appear, cranial neural crest cells at the hindbrain level migrate in distinct, segregated streams that emerge lateral to even-numbered rhombomeres, leaving regions adjacent to odd-numbered rhombomeres void of neural crest cells (Farlie et al., 1999; Guthrie 1996). These migratory streams of neural crest cells fill up the branchial arches, which are ectodermal pouches in the periphery that are also segmented structures. Hindbrain cranial neural crest cells form a good system to study how early segmentation, migration, and later patterning events are related.

One of the major questions in cranial neural crest cell patterning in the hindbrain is what mechanisms shape individual cells into three stereotypical migratory streams that accurately target precise peripheral destinations. The accuracy of the migratory streams is critical to embryonic patterning; the cranial neural crest cells give rise to cartilage and bone of the face, pigment cells, and neurons and glia of the peripheral nervous system (Le Douarin and Kalcheim, 1999). One of the most widely studied neural crest cell streams emerges from rhombomere 4 (r4) because it is adjacent to two neighboring neural—crest-free zones by r3 and r5, and is visually distinguishable. Lineage tracing studies in

mouse, zebrafish, and chick have shown that the r4 stream is a mixture of neural crest cells from r3, r4, and r5 (Sechrist et al., 1993; Schilling and Kimmel, 1994; Birgbauer et al., 1995; Kontges and Lumsden, 1996; Trainor and Krumlauf, 2000). Time-lapse recordings show that chick neural crest cells from r3 and r5 migrate to neighboring rhombomeres in the neural tube and along diagonal trajectories to join the neighboring streams (Kulesa and Fraser, 1998).

The mechanisms by which the neural crest exclusion zones adjacent to the odd-numbered rhombomeres are generated and their function in segregating neural crest cells into distinct streams remains to be resolved. Over the last two decades, there has been some debate concerning how the distinct neural crest cell migratory streams are established. Intrinsic cues in the neural crest cells themselves are one possible mechanism for setting up this pattern. Neural crest cells express genes that are expressed segmentally in the hindbrain, such as members of the Hox and Eph/ephrin family (reviewed in Lumsden and Krumlauf 1996), and there is evidence to suggest that they may be able to impart their segmental cues on overlying surface ectoderm in the branchial arches (Hunt et al. 1991). Intrinsic cues could be genetically programmed into the premigratory neural crest cells within the neural tube and later guide their migration through the periphery.

Extrinsic cues in the peripheral environment form another possible mechanism for the segregated pattern of cranial neural crest cell migration. When chick neural crest cells venture into the regions lateral to the r3 and r5 rhombomeres, the cells either stop and collapse filopodia or divert to join the r2,

r4, or r6 stream (Kulesa and Fraser, 1998). Transplanted cells from grafts of quail r2 or r4 into the r3 or r5 paraxial mesoderm diverge towards neighboring streams, which also supports the presence of local repulsive cues in the regions lateral to r3 and r5 (Farlie et al., 1999). In addition, grafted neural crest cells are able modulate Hox gene expression and migrate according to their new location (Trainor et al., 2002), which shows that their positional genetic identity can be regulated. These studies show that extrinsic cues are also responsible for guiding cranial neural crest cells during their migration.

The current view is that cranial neural crest cells are guided by a combination of intrinsic cues set up in the neural tube and extrinsic cues as cells emerge and interact with each other and the environment (reviewed in Trainor and Krumlauf, 2001). The molecular mechanisms that set up the local repulsive cues in the cranial mesenchyme may originate from the neuroepithelium. When chick r3 neuroepithelium is removed, neural crest cells invade the area adjacent to r3 (Golding et al., 2002, 2004). Recently, semaphorin/neuropilin signaling within rhombomeres at levels adjacent to neural crest cell free zones has been implicated as one of the possible mechanisms restricting neural crest cell streaming lateral to r3 and r5 (Osborne et al., 2005; Yu and Moens, 2005). Thus, individual neural crest cells may interpret local microenvironmental cues and adjust their cell trajectories.

Neural crest cells are not restricted to migration within stereotypical pathways. Time-lapse recordings show that neural crest cells can leave a stream, migrate through an exclusion zone, and contact cells from a neighboring

stream (Kulesa and Fraser, 2000). In a more dramatic and collective way, subpopulations of cranial neural crest cells can compensate for missing, ablated neighbors (Saldivar et al., 1997). Following the ablation of dorsal r5 and r6 in 10-12 somite stage chick embryos, some r4 neural crest cells migrate into the depleted third branchial arch and up-regulate *Hoxa-3*, a transcript they do not normally express (Saldivar et al., 1997). In ovo time-lapse analysis reveals that neural crest cell trajectories are rerouted away from stereotypical migratory pathways towards depleted branchial arches (Kulesa et al 2000). The rerouting of neural crest cell streams is also seen in *Xenopus* embryos when cell-cell contact-mediated cues are perturbed. When the function of certain Eph/ephrin molecules is inhibited, neural crest cells en route to the third branchial arch divert to the second and fourth branchial arches (Smith et al., 1997). While these studies suggest that neural crest cell migratory pathways are plastic and neural crest cells can retarget a new location, especially in response to large genetic or physical perturbations, it is still not understood how individual cells change their migratory behavior. A tremendous challenge for developmental biologists studying neural crest cell patterning is to test the role of potential guidance cues and simultaneously monitor the dynamic spatio-temporal results within intact embryos.

In order to characterize and to understand how the migration of individual cells is altered due to changes in the environment, we challenged the cranial neural crest cell's ability to accurately pathfind by disrupting the local environment along a migratory route. We place physical barriers in the chick

mesoderm, lateral to r4 and prior to the emergence of the r4 neural crest cell stream. By combining time-lapse imaging after the perturbation is introduced, we can uniquely assay neural crest cell migratory behaviors in response to the perturbation in living chick embryos. We focus on the migratory stream lateral to r4 since this stream is easily accessible to manipulation and time-lapse confocal imaging. We find that the majority of neural crest cells reaches the branchial arch destinations, even when the migratory route is almost completely blocked. Time-lapse analysis reveals a repeatable series of events by which the cells overcome the barriers and end up at the second branchial arch (BA2). Surprisingly, quantitative analyses show that there are differences in cell speed and directionalities for initially blocked cells and follower cells, suggesting a correlation between these quantities and directional movement. Our results support the hypothesis that an individual neural crest cell's trajectory is not pre-determined and suggest that extrinsic cues such as cell-cell and cell-environment cues play an important role in the ability of the neural crest cells to accurately target a peripheral destination.

## ***Materials and Methods***

### *Embryos*

Fertile White Leghorn chick eggs were acquired from a local supplier (Lakeview Farms) and were incubated at 38°C for 36 hours or to approximately the 7-9 somite stage (ss) of development. Eggs were rinsed with 70% ethanol and 3 mL of albumin was removed prior to cutting a window through the shell. A solution of 10% india ink (Pelikan Fount; PLK 51822A143) in Howard Ringer's solution was injected below the blastodisc to visualize the embryos. Embryos were staged according to the criteria of Hamburger and Hamilton (1951), by their number of somites, denoted 10 ss, for example.

### *Fluorescent labeling of premigratory neural crest cells*

Premigratory neural crest cells were labeled by pressure injection of 0.5 ug/ul CM-Dil in an isotonic sucrose solution warmed to 37°C (Molecular Probes C-7000 in 10% EtOH and 90% 0.3 M sucrose) into the neural tube lumen of 7-9 ss embryos. This procedure labels the majority of premigratory neural crest cells along the entire A/P axis. To label premigratory neural crest cells in specific rhombomeres, we applied small focal injections of 5 ug/ul CM-Dil in 100% EtOH. Electroporations were carried out as described in Itasaki et al., 1999. We pressure-injected a DNA construct that drives the expression of cytoplasmic GFP with a chick beta-actin promoter (pca-GFP, 5 µg/µl) into the neural tube lumen of 7-9 ss embryos and used electrodes 5 mm apart to apply 2-3 pulses of 25 V

current across the embryo. This procedure also labels premigratory neural crest cells.

#### *Foil and permeable barrier placement*

A sharp scalpel was used to cut tantalum foil (7.5  $\mu\text{m}$  thick, Goodfellow #TA000280) into approximately 100  $\mu\text{m}$  (length) x 100  $\mu\text{m}$  (height), and 200  $\mu\text{m}$  (length) x 100  $\mu\text{m}$  (height) pieces as measured with a micrometer slide under a dissecting microscope. Fine glass needles were used to create a similarly sized cut adjacent and parallel to the neural tube, lateral to prospective r4, in the embryo. Barriers were positioned into the wound using fine forceps and glass needles. To document barrier position and to verify fluorescent cell labeling, embryos were visualized with a fluorescence dissecting scope (Leica MZFLIII) equipped with a Spot RT Color Camera (Diagnostic Instruments, Inc.). Embryos were re-incubated for either 1 hr before selection for time-lapse imaging or overnight for static imaging.

Permeable barriers approximately 400  $\mu\text{m}$  by 100  $\mu\text{m}$  were cut out from a 0.4  $\mu\text{m}$  pored Millicell-CM cell culture insert (Millipore, Inc.) and placed as described for foil barriers.

#### *Time-lapse Confocal Microscopy*

Fluorescently labeled whole embryo explants were visualized using laser scanning confocal microscopes (Zeiss LSM 410) connected to an inverted compound microscope (Zeiss Axiovert). The whole embryo culture set-up was

the same as described in Kulesa and Fraser, 1998. Briefly, a six-well culture plate (Falcon 3046) was modified by making a hole in the bottom of one of the wells and replacing the plastic with a 25 mm circular glass coverslip (Fisher 48380-080) sealed to the dish with a thin ring of silicone grease (Dow Corning 79810-99). The microscope was surrounded by a heater box, constructed of cardboard pieces taped together and covered with thermal insulation (Reflectix Co., 5/16 inch thick) that enclosed a chick incubator heater (Lyon Electric Co. 115-20) and maintained the cultures at 38°C for the duration of filming. The fluorescent dye, Dil, was excited with the 543-laser line. Images were digitally collected every 2 min and stored on 2 GB Jaz disk (Iomega, Inc.) using the Zeiss LSM software. Images were analyzed with Adobe Photoshop (Adobe, Inc.) and converted into movie format with the image processing and analysis packages, NIH Image 1.60, and ImageJ 1.29 (Rasband and Bright, 1995). Images were globally adjusted for brightness and contrast and processed with a median filter in Adobe Photoshop to reduce noise. Some images had an embossing filter applied to bring out the cells with Adobe Photoshop.

### *Time-lapse Data Analysis and Cell Tracking*

Time-lapse confocal data sets were analyzed using a 2D cell-tracking software program called TRACKIT (updated version of XVTRACK, developed by S. Speicher and J. Solomon, California Institute of Technology). Individual cells are tracked based on similarities in brightness and shape in consecutive frames of the time-lapse series, among other criteria; values for mean velocity and

directionality were calculated for cells that were tracked for at least 90% of the time-lapse session. The directionality of an individual cell is defined as the distance between the start and end position of the cell divided by the total length of the path. A cell that travels in a straight line would have a directionality value of 1. For each set of average velocity and directionality values, the average, the standard deviation, and the standard error of the mean were calculated (Microsoft Excel). To compare values between two populations, we used a statistical program (InStat v3.0a, GraphPad Software, Inc.) to perform unpaired t-tests.

## **Results**

To test the roles of intrinsic versus extrinsic guidance cues and the extent to which cranial neural crest cells can diverge from typical migratory pathways, we blocked migratory routes by placing impermeable, biologically inert tantalum foil barriers parallel to and adjacent to the neural tube, prior to the onset of neural crest cell migration (Figure 2.1a). The barriers are placed in the areas where neural crest cells migrate and form stereotypical migratory streams. If the neural crest cells exclusively use intrinsic guidance cues set up prior to emigration, we would expect that an impermeable barrier placed directly in their normal path of migration should block their migration. Below, we describe the results of monitoring individual cell trajectories and cell migratory behaviors in response to the barriers. We focus on the neural crest cell migratory stream that extends laterally from rhombomere 4 (r4) and refer to this stream as the r4 stream, realizing that it also contains cells from other segments, especially r3 and r5.

### *Neural crest cells migrate around foil barrier and reach branchial arch 2*

Neural crest cells are able to populate branchial arch destinations in embryos that have a foil barrier placed along but not completely blocking the stereotypical pathway (Figure 2.1). Static confocal images taken 18 and 24 hours after barrier placement show some neural crest cells blocked at the barrier (Figure 2.1b, c, arrowhead; Figure 2.1d, e, arrow). The majority of neural crest cells reaches and populates branchial arch 2 (BA2) comparable to normal (Figure 2.1b, b'). Streams of neural crest cells are found around the anterior or

posterior edges of the barrier (Figure 2.1b, c, asterisk; Figure 2.1d, e, asterisk). Some neural crest cells are found directly over a barrier in tissue that grows over the barrier during healing. These streams of neural crest cells are thinner than normal, only about 2-3 cells in width versus 6-7 cells. The streams are also less densely packed (Figure 2.1b, b'). The ability of the neural crest to migrate past the barrier depends on the severity of the block posed by the foil barriers (Figure 2.1f, g). When the r4 migration pathway is 100% blocked, cases where the majority of neural crest cells do not reach the branchial arches are observed (3/7). Otherwise, cranial neural crest cells are able to migrate past a barrier and retarget BA2.

*Neural crest cells overcome a foil barrier in a repeatable sequence of events*

To observe the interactions of neural crest cells and the barrier during the formation of novel migratory pathways, we collected time-lapse confocal recordings. The movies capture a repeatable series of events by which cells encounter a barrier and form novel pathways around it (Figure 2.2). In a typical time-lapse imaging session, neural crest cells at the front of a stream encounter a barrier (Figure 2.2b, magenta colored cell), the stream collapses its filopodia, and it stops (Figure 2.2c). The cells actively explore the barrier by extending processes. The neural crest cells at the front and center of the r4 stream that initially encounter the barrier do not divert or turn from their stereotypical paths and tend to be blocked (Figure 2.2b-e, circled cells). However, this situation changes when later cells arrive at the barrier and migrate around the barrier.

Neural crest cells that follow behind the lead cells initially fill in behind the barrier. At the edges of the barrier, these neural crest cells quickly divert and become the new leaders in a novel migratory pathway around the barrier (Figure 2.2). Other neural crest cells soon follow in this path, forming a new migratory stream. Some neural crest cells actually turn and explore the distal side of the barrier, then continue to migrate towards BA2 (Figure 2.2). The new neural crest cell migratory stream does not coalesce into a dense stream with a wide front, typical of a normal r4 stream (Figure 2.2f). Instead, the new streams are thinner and have smaller fronts. Interestingly, the neural crest cells that divert around barriers do not venture into the regions adjacent to r3 and r5. The paths around the barrier tend to stay close to the barrier. The endogenous repulsive zones adjacent to r3 and r5 are for the most part maintained in the embryos.

*Foil barriers at different positions have different effects on cell migration*

To determine whether the interactions of neural crest cells with barriers induce changes in cell migratory behaviors, we measured average speed and directionality values of individual Dil-labeled neural crest cells (Table 2.1). Each Dil-labeled neural crest cell is identified and tracked over time based on particle shape, brightness, and spatial location. By definition, cells with lower directionality values have more circuitous routes. We find that when a foil barrier blocks just 25% of the r4 pathway, the r4 neural crest cells that encounter the barrier migrate faster and in a more circuitous path. Our cell tracking analysis of these cells show a 38% increase in average velocity and a 68% decrease in

directionality (n=15) when compared to r4 neural crest cells that migrate on the contralateral side of the embryo. In contrast, when a barrier is positioned adjacent to r4 and blocks 80% of the r4 stream migratory pathway, neural crest cells from r3 and r4 do not show significant changes in average velocity or directionality values (Table 2.1, Figure 2.3), despite a significant number of blocked cells. In fact, neural crest cells that encounter an r4 barrier have average velocity and directionality values comparable to those of neural crest cells that do not interact with the barrier.

*Neural crest cells are blocked by a permeable barrier*

To test whether neural crest cells can overcome significant blockage of multiple migratory routes, we implanted permeable barriers that extend from the midbrain caudal to mid-r4. Since foil barriers over 200  $\mu\text{m}$  in length lead to neural tube defects (data not shown), we used permeable barriers. In addition, we labeled the neural crest cells with cytoplasmic GFP to better observe cellular processes in time-lapse movies.

We find that the neural crest cells become trapped very effectively by a permeable barrier. The initial cells do not diverge from their pathway; the r4 stream forms posterior to the barrier while the cells in the r2 stream migrate until they are blocked by the barrier (Figure 2.4b). Follower cells from the r2 stream fill in behind and migrate along the barrier, extending processes. In a typical time-lapse session, one neural crest cell strays from the r4 stream and migrates along the barrier towards the r3 repulsive region and, as expected, collapses filopodia

and stops (Figure 2.4b, red cell). As the time-lapse progresses, a couple other cells also begin stray from the r4 stream (blue cells). Instead of stopping, however, they interact with the stopped cell and migrate along the barrier until they meet and interact with trapped cells from the r2 stream (Figure 2.4c, 2.4d, arrow). Cells from the r4 stream now readily stray from their stereotypical path to BA2 and instead form a new stream of cells behind the barrier. Interestingly, the r3 repulsive zone remains clear (Figure 2.4d, asterisk). This illustrates the ability of the neural crest to migrate and to overcome environmental cues by migrating on top of each other.

## ***Discussion***

One of the underlying questions in vertebrate development is what is the effect of segmentation on a dynamic process such as cell migration. At the hindbrain level, the cranial neural crest cells arise from segmented rhombomeres and migrate out into the periphery to populate branchial arches. The past decade of research has identified a number of new molecules involved in the guidance of cranial neural crest cells. At the same time, progress has been made into understanding precise cell trajectories and cell movements (reviewed in Kulesa et al., 2004). However, we still do not understand how individual cells react to changes in the environment in real-time. In this study, we introduce an inert physical barrier along a chick cranial neural crest migratory route and record individual cell behaviors using time-lapse confocal microscopy. We find that neural crest cells are effective at overcoming foil barriers along stereotypical migratory pathways. Neural crest cells find novel pathways around barriers in a repeatable series of events, which culminates with the re-formation of a migratory stream in which follower cells become new lead cells. Foil barriers placed at r3 affect the directionality and velocity of the r4 subpopulation of neural crest cells, whereas barriers placed at r4 do not, suggesting that the r3 and r4 neural crest cells may interpret environmental cues differently. In addition, when the neural crest cells are blocked by a large permeable barrier, they are able to venture into the r3 repulsive zone by migration along each other. Our results demonstrate the robustness of neural crest cells to respond to changes in the environment and

highlight the importance of cell-cell interactions in overcoming environmental cues.

Neural crest cells are able to reroute around or over physical obstacles along the migratory route. This supports the hypothesis that neural crest cells readily respond to changes in the environment. Our initial results show that although the shape of the migratory stream was altered, the cells still reached their branchial arch target. The foil barrier was able to block a majority of the migrating cells in just a few cases (Figure 2.1). If cell trajectories were governed by intrinsic instructions, we would not expect this level of plasticity or flexibility for a cell to retarget. One would not expect them to find a way around the barrier and could expect to find cells piled up behind the barriers. The ability of cells to redirect migratory pathways agrees with data that cranial neural crest cells can reroute, change Hox gene expression, and differentiate according to new target destinations (Saldivar et al. 1997, Kulesa et al. 2000, Trainor and Krumlauf 2000, Trainor et al 2002, Golding et al. 2002).

Dynamic time-lapse data show a series of events that lead to the formation of a novel pathway around a barrier, suggesting a coordinated response by the cells. Neural crest cells that first encounter a barrier stop and thoroughly explore the barrier and the surrounding environment. Follower cells forge a path around the barrier as individuals, soon followed by other neural crest cells. Local cell-cell interactions occur frequently between leading and following cells. Since neural crest cells have been shown to extend processes for up to 100  $\mu\text{m}$  (Teddy and Kulesa, 2004), it is possible that long distance cell

communication contributes to the plasticity demonstrated by the neural crest cells.

*Lead cells and follower cells are not inherently specific cells within the stream, and can change roles during the course of the migration*

Our experiments perturb the relationship between the lead cells at the fronts of migratory streams and follower cells. Previous studies found that within the r4 stream, neural crest cells at the front, or leaders, tend to migrate with higher directionality and lower velocity than those in the back of the stream, or followers (Kulesa and Fraser, 1998). As is in the case of other types of migration, such as studies of zebrafish commissural axons across a midline (Bak and Fraser, 2003), this suggests that there is a difference in the migratory behavior of leaders and followers. One explanation could be that leader cells play a greater role in detecting guidance cues and exploring the migration route, while cell-cell interactions play more of a role in guiding follower cells. Another possibility is that of population pressure (LeDouarin, 1982; Newgreen et al., 1979), where the follower cells push upon the leader cells and migrate along signals generated by the leader cells. Although population pressure may be responsible for follower cells finding a novel pathway around a barrier, the narrow, less dense, and more directed stream that forms lateral to the barrier is more likely due to cell-cell contact-mediated guidance. Our results show the roles of leaders and followers are not inherent to the cells and can be interchanged during cranial neural crest migration.

*Foil barriers at r3 and r4 have different effects on cell migration*

The r3 surface ectoderm, paraxial mesoderm, and neural tube have been shown to be effective at repulsing cranial neural crest cells and are believed to possess a repulsive cue (Golding et al., 2002; Farlie et al., 1999). We find that r3 cells, regardless of whether they encounter the barrier or not, travel much faster when there is an impermeable barrier at r3 ( $p < 0.05$  for non-barrier cells,  $p < 0.001$  for barrier cells) compared with one at r4. R4 neural crest cells also travel faster when they encounter an r3 barrier than when they do not ( $p < 0.001$ , Table 2.1). In contrast, r4 neural crest cells that encounter an r4 barrier migrate with mean velocity and directionality values similar to those that do not. Taken together, our analyses show that foil barriers at r3 have a stronger effect on the migration of cranial neural crest cells despite not actually blocking the cells very much. The position of the foil barriers may affect the degree to which migration is perturbed by affecting the diffusion or dissipation of a cue. Ablation of the r3 neuroepithelium results in the gradual loss of repulsive cues (Golding et al., 2004). One possibility is that a foil barrier at the r3 is able to block this endogenous repulsive cue lateral to r3, and we are able to detect the resulting changes in migratory behavior.

In our foil barrier experiments, neural crest cells migrate along the barrier and each other, at times venturing close to the edge of repulsive zones, but never going in. This is true even when the migratory pathway is entirely blocked. This is in contrast to our permeable barrier experiment, which shows the cells are

able to mismigrate into the r3 repulsive zone by interacting with each other when the barrier extends completely into the repulsive zones. One possibility is that the permeable barrier disrupts the repulsive cues in the r3 region. For example, neural crest cells also mismigrate and form ectopic ganglia when the r3 exclusion zone is manipulated through an ErbB4 mouse knockout, r3 ablation in chick (Golding et al. 2000, 2002), or Sema3F/G misexpression or knockdown in zebrafish (Yu and Moens, 2005). However, we do not believe this to be the case. The cells still avoid a small crest-free zone directly by r3 and migrate in a dense stream by the barrier. This argues that repulsive cues are still intact immediately adjacent to r3. Our data support the idea that extrinsic guidance cues in the paraxial environment are responsible for sculpting the normally dense shape of the r4.

Our results show that neural crest cell migratory routes can be manipulated en route to the branchial arches by introducing physical barriers in the tissue perpendicular to the direction of the stream migration. Our results suggest that the trajectory a neural crest cell takes is dependent on local guidance cues. If local directional cues are absent or perturbed, neural crest cells have the ability to search for new guidance cues. Future work of neural crest cell guidance mechanisms may have to focus on cell-cell and cell-environment interactions in the microenvironment along the stereotypical migratory routes.

### ***Acknowledgements***

The authors would like to thank R. Krumlauf for the generous gift of the *pca*-GFP construct; M. Basch and M. Bronner-Fraser for the generous gift of tantalum foil. P.M.K. would like to thank the Burroughs Wellcome—funded Computational Molecular Biology Program at Caltech for its generous support during this work. C.C.L. and S.E.F. are supported in part by the Beckman Institute and the NIH.

### ***References***

- Bak, M. and Fraser, S. E.** (2003). Axon fasciculation and differences in midline kinetics between pioneer and follower axons within commissural fascicles. *Development* **130**, 4999-5008.
- Birgbauer, E., Sechrist, J., Bronner-Fraser, M. and Fraser, S.** (1995). Rhombomeric origin and rostrocaudal reassortment of neural crest cells revealed by intravital microscopy. *Development* **121**, 935-45.
- Golding, J. P., Dixon, M. and Gassmann, M.** (2002). Cues from neuroepithelium and surface ectoderm maintain neural crest-free regions within cranial mesenchyme of the developing chick. *Development* **129**, 1095-105.
- Golding, J. P., Sobieszczuk, D., Dixon, M., Coles, E., Christiansen, J., Wilkinson, D. and Gassmann, M.** (2004). Roles of ErbB4, rhombomere-specific, and rhombomere-independent cues in maintaining neural crest-free zones in the embryonic head. *Dev Biol* **266**, 361-72.

**Golding, J. P., Trainor, P., Krumlauf, R. and Gassmann, M.** (2000). Defects in pathfinding by cranial neural crest cells in mice lacking the neuregulin receptor ErbB4. *Nat Cell Biol* **2**, 103-9.

**Guthrie, S.** (1996). Patterning the hindbrain. *Curr Opin Neurobiol* **6**, 41-8.

**Hamburger, V. and Hamilton, H. L.** (1951). A series of normal stages in the Development of the chick embryo. *J Morphology* **88**, 49-92.

**Hunt, P., Wilkinson, D. and Krumlauf, R.** (1991). Patterning the vertebrate head: murine Hox 2 genes mark distinct subpopulations of premigratory and migrating cranial neural crest. *Development* **112**, 43-50.

**Itasaki, N., Bel-Vialar, S. and Krumlauf, R.** (1999). 'Shocking' Developments in chick embryology: electroporation and in ovo gene expression. *Nat Cell Biol* **1**, E203 - E207.

**Kontges, G. and Lumsden, A.** (1996). Rhombencephalic neural crest segmentation is preserved throughout craniofacial ontogeny. *Development* **122**, 3229-42.

**Kulesa, P., Ellies, D. L. and Trainor, P. A.** (2004). Comparative analysis of neural crest cell death, migration, and function during vertebrate embryogenesis. *Dev Dyn* **229**, 14-29.

**Kulesa, P. M. and Fraser, S. E.** (1998). Neural crest cell dynamics revealed by time-lapse video microscopy of whole embryo chick explant cultures. *Dev Biol* **204**, 327-44.

- Kulesa, P. M. and Fraser, S. E.** (2000). In ovo time-lapse analysis of chick hindbrain neural crest cell migration shows cell interactions during migration to the branchial arches. *Development* **127**, 1161-72.
- Le Douarin, N. and Kalcheim, C.** (1999). *The Neural Crest*, 2nd ed. Cambridge: Cambridge University Press.
- Lumsden, A. and Krumlauf, R.** (1996). Patterning the vertebrate neuraxis. *Science* **274**, 1109-15.
- Newgreen, D. F., Ritterman, M. and Peters, E. A.** (1979). Morphology and behaviour of neural crest cells of chick embryo in vitro. *Cell Tissue Res* **203**, 115-40.
- Osborne, N. J., Begbie, J., Chilton, J. K., Schmidt, H. and Eickholt, B. J.** (2005). Semaphorin/neuropilin signaling influences the positioning of migratory neural crest cells within the hindbrain region of the chick. *Dev Dyn* **232**, 939-49.
- Rasband, W. S., Bright, D.S.** (1995). NIH Image: A public domain image processing program for the Macintosh. *Microbeam Analysis* **4**, 137-149.
- Sadaghiani, B. and Thiebaud, C. H.** (1987). Neural crest development in the *Xenopus laevis* embryo, studied by interspecific transplantation and scanning electron microscopy. *Dev Biol* **124**, 91-110.
- Saldivar, J. R., Sechrist, J. W., Krull, C. E., Ruffins, S. and Bronner-Fraser, M.** (1997). Dorsal hindbrain ablation results in rerouting of neural crest migration and changes in gene expression, but normal hyoid development. *Development* **124**, 2729-39.

- Schilling, T. F. and Kimmel, C. B.** (1994). Segment and cell type lineage restrictions during pharyngeal arch development in the zebrafish embryo. *Development* **120**, 483-94.
- Sechrist, J., Serbedzija, G. N., Scherson, T., Fraser, S. E. and Bronner-Fraser, M.** (1993). Segmental migration of the hindbrain neural crest does not arise from its segmental generation. *Development* **118**, 691-703.
- Smith, A., Robinson, V., Patel, K. and Wilkinson, D. G.** (1997). The EphA4 and EphB1 receptor tyrosine kinases and ephrin-B2 ligand regulate targeted migration of branchial neural crest cells. *Curr Biol* **7**, 561-70.
- Teddy, J. M. and Kulesa, P. M.** (2004). In vivo evidence for short- and long-range cell communication in cranial neural crest cells. *Development* **131**, 6141-51.
- Trainor, P. A. and Krumlauf, R.** (2000). Patterning the cranial neural crest: hindbrain segmentation and Hox gene plasticity. *Nat Rev Neurosci* **1**, 116-24.
- Trainor, P. A. and Krumlauf, R.** (2001). Hox genes, neural crest cells and branchial arch patterning. *Curr Opin Cell Biol* **13**, 698-705.
- Vaage, S.** (1969). The segmentation of the primitive neural tube in chick embryos (*Gallus domesticus*). A morphological, histochemical and autoradiographical investigation. *Ergeb Anat Entwicklungsgesch* **41**, 3-87.
- Yu, H. H. and Moens, C. B.** (2005). Semaphorin signaling guides cranial neural crest cell migration in zebrafish. *Dev Biol* **280**, 373-85.

## Figures

### *Figure 2.1: Foil barriers are ineffective at blocking cranial neural crest*

(1a) A typical 10 ss chick embryo with a foil barrier inserted adjacent to r4. The Dil channel is merged with the bright field image in 1b and 1d, or shown alone in 1c and 1e. (1b, c) 18 hours later, the neural crest cells in the r4 stream have been able to migrate to BA2 by migrating around (asterisk) or over (arrowhead) the barrier. (1d, e) The r4 stream (asterisk) has migrated posterior to the barrier to BA2, but there is a pileup of blocked neural crest cells from r2 (arrow). (1f) The r4 pathway lies between lines drawn at the r3/r4 and the r4/r5 boundary. Percent r4 blocked is the part of the region blocked by the foil barrier. (1g) 18-24 hr after barrier placement, migration is categorized as: around, neural crest cells (NCCs) migrate anterior or posterior of the barrier; around & over, NCCs also migrate dorsally over the barrier; over, NCCs migrate only over the barrier; and stopped, NCCs are blocked by the barrier and there are no Dil-positive cells in BA2. Each circle denotes one embryo (n=21). OV, otic vesicle; BA2, branchial arch 2; BA3, branchial arch 3; BA4, branchial arch 4; scalebars are 100  $\mu\text{m}$ .



*Figure 2.2: Leaders and followers change when a population of neural crest cells encounters a barrier*

We examined the differences in cell behavior by neural crest cells (NCCs) as they meet a barrier at r4. (2a) The Dil channel has been embossed and merged with the bright field image of the embryo. Lines are drawn at the boundary between different rhombomeres. 80% of r4 is blocked by the barrier (asterisk). The region within the gray square is enlarged in 2b to 2j. (2b) 1 hr 19 min later one cell (magenta) migrates laterally from r4, hits the barrier (dark rectangle), collapses its filopodia in 2c, and continues to be blocked until it is out of focus. (2c) At 3 hr 27 min, NCCs find a way around the posterior portion of the barrier (asterisk). Other NCCs begin to migrate away from the neural tube toward the anterior part of the barrier (yellow, blue, orange cells) and onto BA2 in 2d to 2e. (2d) Note that the yellow cell has overtaken the blue cell around the barrier, and briefly explores the opposite side of the barrier. Meanwhile, the NCCs (red, light blue) that hit the middle of the barrier are blocked. (2e) At the end of the movie, one cell (white outline) is able to find a way over the barrier. (2f) A Z-projection of the time-lapse shows cumulative NCC migratory pathways. r4, rhombomere 4. 100  $\mu\text{m}$  scalebars.

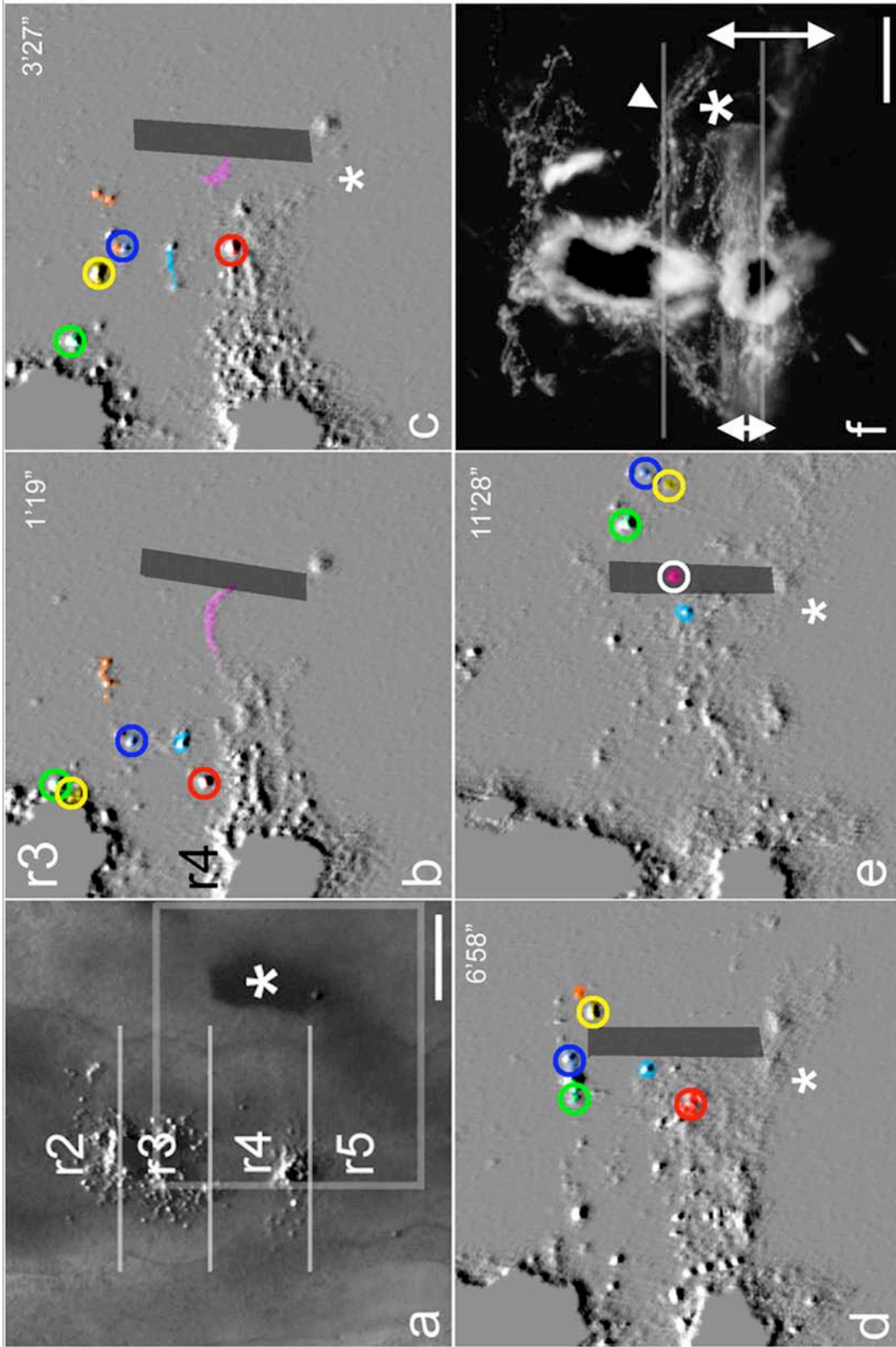


*Figure 2.3: Neural crest cells that are blocked behind the barrier tend to migrate faster than cells that go around the barrier*

An embryo with a foil barrier placed at r4 and focally labeled premigratory neural crest cells at the r3 and r4/r5 boundary was time-lapsed. (3a) On a scatter plot, the directionality and mean velocity values of migrating neural crest cells loosely segregates the cells into two populations: cells that displayed relatively high directionality, low velocity values (blue box); and cells that had a low directionality, high velocity values (red box). Differences in mean velocity and directionality values between these two populations were statistically different in an unpaired t-test; see text. To see whether these characteristics corresponded to different populations of migrating neural crest cells, we looked at the paths. (3b) Neural crest cells trapped behind the barrier tend to fall into the high mean velocity but low directionality subpopulation (red). r3 or r4 barrier refers to the neural crest cells that migrated out from r3 or r4 to the barrier side; r3 or r4 non-barrier refers to neural crest cells that migrate to the other side; r4, rhombomere 4; asterisk, position of the barrier.

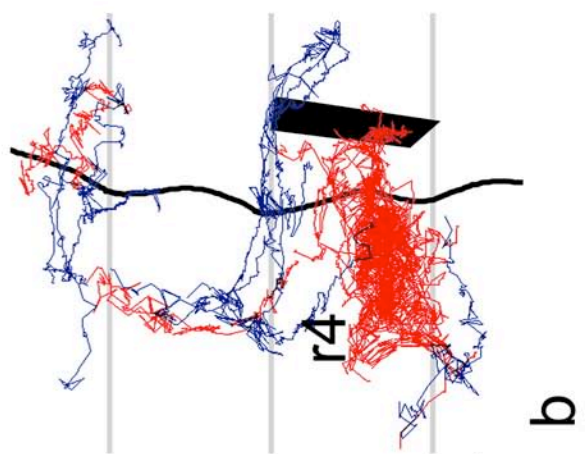
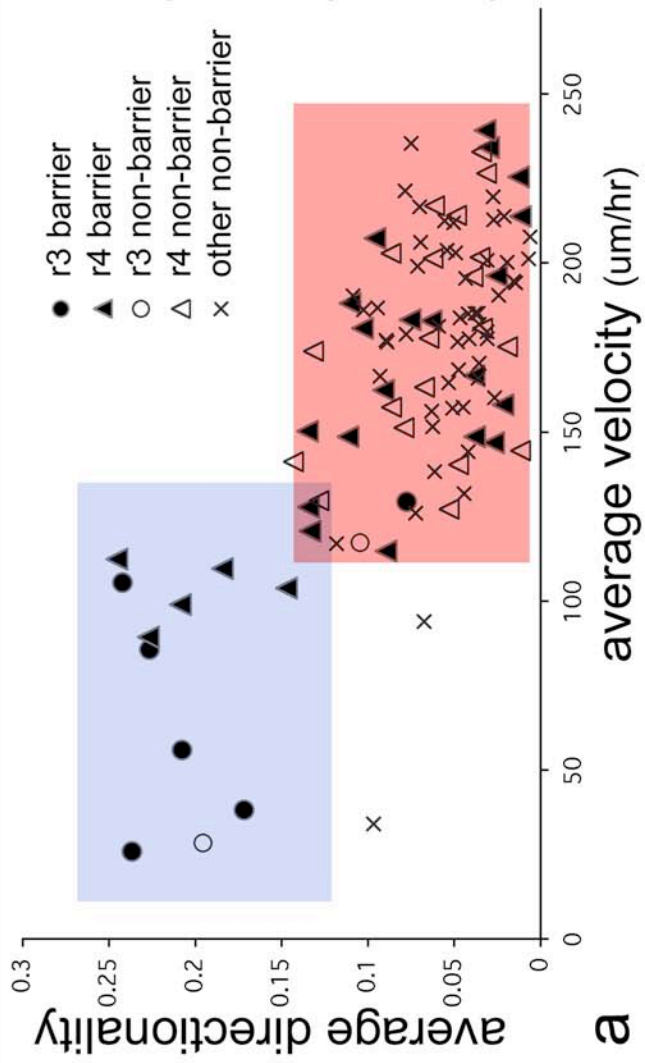


*Figure 2.4: Neural crest cells are able to migrate into the r3 repulsive zone by migrating on top of each other*

An embryo was electroporated with a DNA-expressing cytoplasmic GFP on the right side, and a permeable barrier with 0.4  $\mu\text{m}$  pores was placed adjacent to the neural tube. (4a) At the start of the time-lapse some r4 neural crest cells have reached the barrier (arrowhead), and other neural crest cells at the level of r1/2 are migrating along the barrier. Box shows the boundary of region shown in 4b, c and d. (4b) 4 hours later, the r4 stream has formed posterior to the barrier, and more cells have piled up behind the barrier at the r1/2 level, some migrating posteriorly along the barrier (2 cells, blue). Two cells diverge from the r4 stream (red, yellow, arrow). (4c, 4d) 18 minutes later, the yellow cell (arrow) overtakes the red cell and contacts r2 cells behind the barrier in 4d. The r3 region remains free of neural crest cells (asterisk).

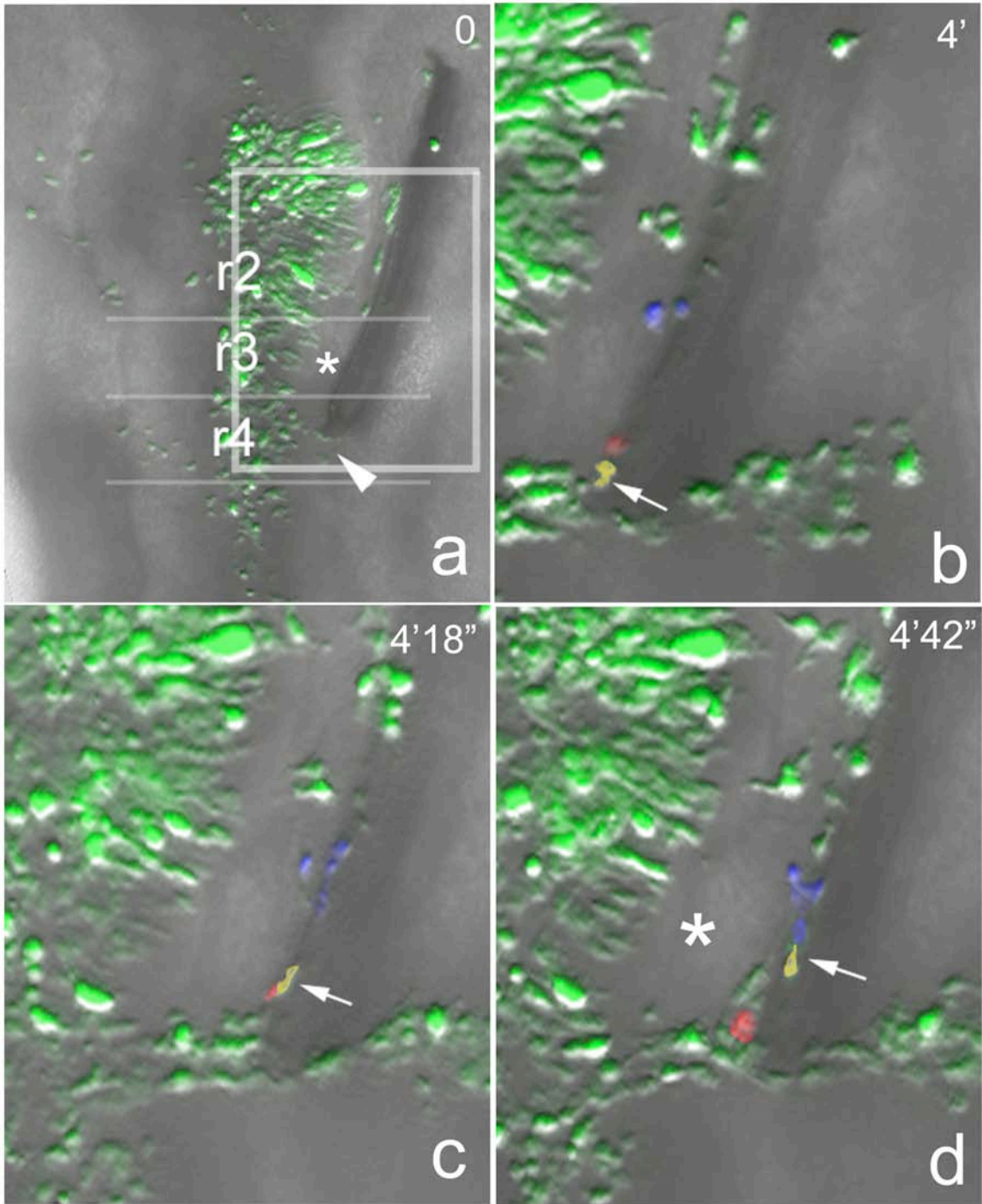


Table 2.1: Mean velocity and directionality for barriers at r3 and r4

Movie	%r3 %r4 blocked		Labeled cells	Encounters Barrier	Velocity (um/hr $\pm$ SD)	Directionality ( $\pm$ SD)	n	Velocity $\Delta$	Directionality $\Delta$		
1	8%	80%	r3	+	74 $\pm$ 40	0.19 $\pm$ 0.06	6	1%	27%		
				-	73 $\pm$ 63	0.15 $\pm$ 0.06	2				
			r4	+	164 $\pm$ 43	0.09 $\pm$ 0.06	24			- 8%	50%
				-	178 $\pm$ 33	0.06 $\pm$ 0.04	20				
			r3 & r4	+	146 $\pm$ 55	0.11 $\pm$ 0.08	30			- 14%	57%
				-	169 $\pm$ 46	0.07 $\pm$ 0.05	22				
3	75%	23%	r3	+	152 $\pm$ 5	0.06 $\pm$ 0.02	6	- 2%	0%		
				-	155 $\pm$ 39	0.06 $\pm$ 0.03	44				
			r4	+	153 $\pm$ 37	0.10 $\pm$ 0.03	15			38% *	- 68% **
				-	111 $\pm$ 25	0.31 $\pm$ 0.07	9				
			r3 & r4	+	153 $\pm$ 40	0.09 $\pm$ 0.03	21			3%	- 18%
				-	147 $\pm$ 40	0.11 $\pm$ 0.10	53				
4	73%	25%	r3 & r4	+	217 $\pm$ 27	0.06 $\pm$ 0.02	17	18%	- 25%		
				-	183 $\pm$ 53	0.08 $\pm$ 0.04	28				

\* p=0.003, t=3.354, unpaired t-test with Welch's correction

\*\* p<0.0001, t=8.542, unpaired t-test with Welch's correction

Barriers were positioned at r3 or r4. Premigratory neural crest cells in r3 and/or r4 were focally labeled with Dil and tracked. Neural crest cells either encountered the barrier (+) or did not (-), for example, if they were cells that migrated to the opposite side of the barrier. The average velocity and directionality of each subpopulation is shown along with standard deviations based on the number of

cells tracked (#) in each population. Differences in velocity and directionality are for the barrier cells when compared to non-barrier cells.

### **CHAPTER 3: Time-lapse analysis of perturbations of ephrin-A5 and EphA4 during cranial neural crest migration in the avian embryo**

Manuscript in preparation.

#### ***Abstract***

Cranial neural crest cells migrate away from the hindbrain in three discrete streams adjacent to even-numbered rhombomeres, rhombomere 2 (r2), r4, and r6. The r6 stream is formed by post-otic neural crest cells that emigrate from r6, r7, and the first few somites. The neural crest cells first form a field of cells lateral to the hindbrain that then segregates between BA3 and BA4. Here we investigate the role of ephrin-A5 and EphA4 during the migration of BA3 and BA4 neural crest cells. We find that ectopic expression of ephrin-A5 specifically causes the r6 subpopulation of neural crest cells to have truncated migration. By conducting time-lapse confocal microscopy and cell-tracking analysis, we find that ectopic ephrin-A5 does not affect directionality, suggesting that transfected r6 neural crest cells are able to properly follow guidance cues. Ectopic expression of constitutively active, truncated EphA4 causes neural crest cells to migrate aberrantly around the otic vesicle. Our cell-tracking analysis finds that ectopic EphA4 activity causes erratic migratory behavior in neural crest cells. Pathfinding errors are accompanied by changes in migratory behavior, with the neural crest cells migrating much faster but with less directionality than normal. Lastly, we find

that expression of a truncated, kinase-dead version of EphA4 also leads to pathfinding errors. Our results suggest that ephrin activity is likely involved in the cessation of migration, whereas Eph activity is involved in pathfinding, and maintenance of migration.

## ***Introduction***

The role of cell movements during embryological development is largely one of context. The coordination of cellular identity with spatio-temporal location is crucial to the organization and formation of tissues and organs. Precise cell movements are important in ensuring that cells reach correct destinations in a timely fashion in order to contribute properly to tissues and structures. Changes in either migratory pattern or cell specification could result in significant structural differences in the future embryo. How migratory cells interpret cues in the extrinsic environment for proper pathways is not well understood. Neural crest cells are a good system to address questions about migration because they undergo extensive migration and give rise to a variety of cell types throughout the vertebrate embryo.

The neural crest is specified early during the developmental process from interactions between the prospective ectoderm and neuroectoderm. The process of specification involves many signaling pathways including Wnts, BMPs, FGFs (reviewed in Barembaum and Bronner-Fraser, 2005; Basch et al., 2004; Cornell and Eisen, 2005; Morales et al., 2005; Raible and Ragland, 2005; Steventon et al., 2005). Many of the genes up-regulated during specification are also involved in migration (Gammill and Bronner-Fraser, 2002), suggesting that the premigratory neural crest cells are actively primed for migration. In the avian embryo, the neural crest cells undergo an epithelial to mesenchymal transition and emerge individually from the dorsal neural tube. This transient population of neural crest cells can be divided up into several subpopulations according to

where they emerge along the anteroposterior axis: cranial, sacral, cardiac, trunk. The cranial neural crest gives rise to cranial ganglia, connective tissues, cartilage, and bone (Le Douarin and Kalcheim, 1999).

The cues involved in the guidance of migrating neural crest cells are actively investigated. Both trunk and cranial neural crest cells migrate in a segmented manner, with areas of migratory neural crest cells separated by crest-free regions. In the trunk, the neural crest cells migrate through the anterior portion of the somite and avoid the posterior portion (Bronner-Fraser, 1986; Rickman et al., 1985; Serbedzija et al., 1990). This segmental migration is guided by permissive cues in the anterior portion of the somite and repulsive cues in the posterior portion of the somite. Signaling pathways shown to pattern trunk neural crest migration include the Eph/ephrin signaling pathway (Krull et al. 1997; Wang and Anderson, 1997; Krull 1998) and PNA binding proteins (reviewed in Krull 1998). Recent studies have demonstrated the requirement of neuropilin 2/semaphorin 3F (Gammill et al., 2006). Trunk neural crest cells migrate through both portions of the somites in neuropilin 2 or semaphorin 3F mutants (Gammill et al., 2006).

Cranial neural crest cells also migrate in a segmented pattern. The premigratory neural crest cells arise from the dorsal aspect of the hindbrain and migrate in three discrete pathways that extend laterally from even-numbered rhombomeres, rhombomere 2 (r2), r4, and r6 to lateral branchial arches 2 (BA2), BA3, and BA4. These streams of migratory neural crest cells are separated by crest-free zones adjacent to r3 and r5. Neural crest cells from r3 and r5 join the

r2, r4, or r6 neural crest cells (Kulesa and Fraser, 1998a; Sechrist et al., 1993; Serbedzija et al., 1992; Trainor et al., 2002). The segmented pattern of migration is thought to be important for properly patterning craniofacial structures by maintaining the segmental identity of cranial neural crest cells (Ellies et al., 2002; Kontges and Lumsden, 1996).

The genes that pattern cranial neural crest migration are largely unknown. The r4 stream is buffered by two crest-free zones where repulsive cues from r3 and r3 surface ectoderm, such as ErbB4, help shape the pathway (Golding et al., 2004; Golding et al., 2000). Neural crest cells within the r4 stream migrate directly away from r4 in a dense, tight pathway (Kulesa and Fraser 1998a; Kulesa and Fraser 2000, personal observation). The formation of the r6 stream is less constrained. Post-otic neural crest cells emerge from r6, r7, and the first few somite levels and first form a field of cells lateral to the hindbrain that then segregates between BA3 and BA4. In *Xenopus*, where the cranial neural crest cells first emerge in a wave that segregates into discrete streams, the ectopic expression of ephrin-B2, and either truncated or kinase-dead Eph receptors, causes third arch neural crest cells to mismigrate into adjacent streams and reveals a role for Eph/ephrin in segregating the streams (Helbling et al., 1998; Smith et al., 1997). In mouse, ephrin-B1 reverse signaling has also been shown to be required cell-autonomously within the cranial neural crest cells for proper migration into branchial arch 3 (BA3) and BA4 (Davy et al., 2004). Whether the Eph/ephrin signaling pathway is also involved in avian cranial neural crest migration is currently not known.

Here we show that ephrin-A5 and EphA4 are expressed at the right time and place to be candidate guidance cues for cranial neural crest migration in the posterior hindbrain. We perturb the Eph/ephrin signaling pathway within the migratory neural crest cells by ectopic expression of full-length ephrin-A5, a truncated, constitutively active intracellular domain of EphA4 (EphA4(int)), as well as a kinase-dead version of the truncated EphA4 (EphA4(kd)), which is believed to act in a dominant negative manner. We find that ectopic expression of ephrin-A5 specifically causes the r6 subpopulation of neural crest cells to cease migration prematurely. By conducting time-lapse confocal microscopy and cell-tracking analysis, we find that ectopic ephrin-A5 does not affect directionality, suggesting that transfected r6 neural crest cells are able to properly follow guidance cues. Ectopic expression of both EphA4(int) and EphA4(kd) causes neural crest cells to migrate aberrantly around the otic vesicle. Ectopic EphA4 activity causes erratic migratory behavior in neural crest cells. Pathfinding errors are accompanied by changes in migratory behavior, with the neural crest cells migrating much faster but with less directionality than normal. Our results support multiple roles for Eph/ephrin signaling during cranial neural crest cell migration, including regulation of the extent of migration in addition to guidance.

## **Materials and Methods**

### *Electroporation and focal Dil labeling of Avian Embryos*

Fertile hen eggs obtained from a local farm (Chino Valley Ranchers, Arcadia, CA) were incubated to 7-9 ss, or 36 hrs, in a humidified 37°C incubator. The eggs were misted with 70% ethanol and then 3 mL of thin albumin was removed with an 18.5 gauge needle (Becton Dickinson & Co, Franklin Lakes, NJ). A window was cut into the shell and a solution of 0.01% FD&C Blue 1 (#CAS 3844-45-9, Spectra Colors Corp, Kearny, NJ) in Howard Ringer's solution was injected below the blastodisc to visualize the embryos. In our hands, this greatly enhanced survival during electroporation as compared with india ink (J. Kastner, personal communication). Embryos were staged by the number of somites, denoted 10ss for example, and other anatomical features according to the criteria of Hamburger and Hamilton (1951).

Electroporations were carried out as previously described (Itasaki et al., 1999; Krull and Kulesa, 1998; Momose et al., 1999). Briefly, plasmid DNA was pressure-injected into the lumen of the neural tube using a picospritzer and a pulled quartz micropipette with a filament. Parallel platinum electrodes were placed 5 mm apart and three 50 ms pulses of 20 V were applied across the embryo. The embryos were then sealed with tape and allowed to recover in an incubator prior to time-lapse microscopy or antibody staining. Note that only the right side of the neural tube is electroporated to maximize the level of labeling on that side as the embryo turns during time-lapse sessions.

Focal Dil injections were carried out to label rhombomere-specific populations of premigratory neural crest cells. A small amount of CM-Dil 5 ug/ul in ethanol (C7000 Molecular Probes) was pressure-injected into the dorsal region of r6.

### *Constructs*

pca-EGFP (4 ug/ul, gifted by R. Krumlauf) was used to express cytoplasmic EGFP via a chick beta-actin promoter and cmv enhancer. pmes-Ephrin-A5 (3 ug/ul, gifted by C. Krull) expresses full-length Ephrin-A5 along with IRES-EGFP from a bicistronic mRNA (Eberhart et al., 2002; Swartz et al., 2001). pca-EphA4(int) and pca-EphA4(kd) drives the expression of the intracellular domain of EphA4 fused to membrane-tagged GFP under the chick beta-actin promoter. Constructs were subcloned using PCR from constructs #167 and #168 gifted by Q. Xu.

### *In situ hybridization*

Wholemout in situ hybridizations with probes to Ephrin-A5 (Baker and Antin, 2003), gifted by R. Baker and P. Antin, and EphA4 (Becker et al., 1995) were carried out as described (Wilkinson, 1992) with slight modifications (H. McBride, personal communication). Select whole mounts were cryoprotected in 15% sucrose, embedded in gelatin, and cryosectioned into 15  $\mu$ m sections. Whole-mount and sections were imaged with an Axiocam, a color digital CCD camera, attached to an Axiophot microscope (Zeiss, Inc., Germany).

### *Immunohistochemistry*

Embryos were fixed in 4% PFA, washed in PBS with 0.1% TX-100 (PBT) to enhance penetration, and blocked in 10% heat-inactivated sheep serum in PBT. Primary antibodies were applied as follows in PBT with 5% serum: mouse monoclonal antibody against Hnk-1 (1:10), rabbit polyclonal antibody against phospho-histone 3 (1:200, #06-570 Upstate Biotechnology, Inc.), rabbit antibody against EphA4 (1:1000, gifted by E. Pasquale, Soans et al., 1996), rabbit polyclonal antibody against Dlx (1:100, Panganiban et al., 1995), gifted by S. Bhattacharyya), rabbit polyclonal antibody against Ephrin-A5 (1:500, #38-0400 Zymed, Inc.), and mouse anti-GFP antibody (1:100, #A11120, Molecular Probes, Inc). Anti-mouse or -rabbit secondary antibodies conjugated with Cy3, Cy5, and FITC dyes were applied at 1:400 (Jackson Labs).

### *Time-lapse Microscopy and Analysis*

Fluorescently labeled embryos were explanted for imaging as described previously (Krull and Kulesa, 1998; Kulesa and Fraser, 1998). The embryo was dissected with an O-ring cut out of filter paper for support, into warmed Howard Ringer's buffer. The embryo was placed dorsal side down onto a fibronectin-coated (20 ug/mL, F2006 Sigma) cell culture insert (PICM03050, Millipore, Inc). Excess liquid was removed to allow the embryo to spread out. The insert was then placed inside a humidified and warmed six-well plate (3046, Falcon, Inc) with added Neurobasal medium supplemented with 2% B27 (#17504-036,

GIBCO), 1% L-Glutamine (G-3126 Sigma), and 1% Pen-Strep (GIBCO). The bottom of the well has a 20 mm diameter drilled hole that was covered by a 25 mm diameter circular glass coverslip (Fisher 48380-080), sealed on with silicone grease (#79810-99, Dow Corning). This allows imaging from the bottom. The sides of the chamber were sealed with tape to prevent evaporation.

An inverted confocal microscope (either a Zeiss 410 or Pascal) was insulated by a custom fit heater box constructed out of cardboard surrounded by thermal insulation (8 mm thick, Reflectix Co.) and heated to 37°C by a chick incubator (#115-20 Lyon Electric Co., Inc.) attached to a temperature regulator. A 10x Plan-Apochromat objective with a 0.45 NA was used to collect 5 z-sections at 20 um to 25 um intervals every 1.5 minutes. ImageJ 1.32j (Rasband and Bright, 1995) was used to project z-sections at each time point into one image, and this XYT data set was aligned using TurboReg and StackReg plugins (Thévenaz et al., 1998). Adobe Photoshop 7.0 (Adobe Systems, Inc.) was used to globally adjust brightness and contrast. Cell-tracking analysis was done using Imaris (Bitplane AG, Zurich, Switzerland). Visualization tools from Zeiss' LSM software (Zeiss, Inc., Germany) were also used. Statistical analyses were carried out using Prism 4.0b (GraphPad, Inc., San Diego, CA), and Excel v.X (Microsoft, Seattle, WA).

## **Results**

### *EphA4 and ephrin-A5 show overlapping expression by rhombomere 6 (r6) and non-overlapping expression by r4 axial levels of the hindbrain*

In the avian embryo, cranial neural crest cells begin to emigrate from the hindbrain at HH9. By HH11, there are streams of migrating neural crest cells that extend from the even-numbered rhombomeres to their branchial arch destinations (Guthrie, 1996). We examined the expression pattern of EphA4 and ephrin-A5 at this stage to investigate whether they may play a role during the migration of the cranial neural crest cells. EphA4 is expressed in the neural tube from the r4 to r6 level and in the otic vesicle (Figure 1). At later stages the expression of EphA4 declines in r4 and focuses at r3 and r5 (data not shown). At the rhombomere 4 (r4) level during HH11, EphA4 and ephrin-A5 are expressed in non-overlapping domains (Figure 1C, 1I arrowhead), with EphA4 in the surface ectoderm adjacent to the neural tube. Ephrin-A5 is expressed in the mesenchyme, coincident with actively migrating neural crest cells. Both EphA4 and ephrin-A5 are expressed in the r6 mesenchyme (Figure 1E, 1J), also coincident with migrating neural crest cells. Our data show that both EphA4 and ephrin-A5 are expressed at the right time and place to play a role in cranial neural crest migration.

### *Ectopic ephrin-A5 initially leads to fewer cells in BA3*

Ephrin-A5 is expressed in r4 and r6 mesenchyme and overlaps with migrating neural crest cells, which supports a potential role in the migration of the

neural crest cells in the r4 and r6 streams. To test this possibility we examined the effects of ectopic ephrin-A5 expression in migrating neural crest cells. We electroporated premigratory neural crest cells with pmes-ephrin-A5, a construct that contains an IRES and drives the expression of both full-length ephrin-A5 and EGFP under a chick beta-actin promoter (Swartz et al., 2001). Cells that are GFP positive also express ectopic levels of ephrin-A5, hereto referred to as ephrin-A5+/GFP+. Within 8 hours post-electroporation, at HH10+, ephrin-A5+/GFP+ cranial neural crest cells can be seen migrating away from the neural tube (Figure 2A, 2A'). They contribute extensively to the r4 stream (Figure 2A', arrow), which forms normally between crest-free zones at r3 and r5. In contrast, few ephrin-A5+/GFP+ cells are seen at the r6 level (Figure 2A', asterisk) despite uniformity in labeling along the neural tube. There is also extensive migration from r7 and the neural tube at the level of the first few somites. By HH13+, ephrin-A5+/GFP+ neural crest cells fully populate branchial arch 1 (BA1), BA2, and BA4. In contrast, there are fewer ephrin-A5+/GFP+ cells in BA3 (Figure 2B, 2B' asterisk). By HH16 there is even distribution of neural crest cells within BA3 (Figure 2C, 2C'). Neural crest cells expressing ectopic levels of ephrin-A5 are disproportionately absent from BA3.

#### *Neural crest cells ectopically expressing EphrinA5 do not migrate to BA3*

To better characterize the extent of migration (or lack thereof) we targeted premigratory neural crest cells by electroporation of either pmes-ephrin-A5 or pca-EGFP constructs into the lumen of the neural tube, and then stained the

embryos with antibodies against HNK-1, a carbohydrate moiety commonly used as a marker for migrating neural crest cells. Control embryos were electroporated with *pca*-EGFP, a construct that drives the expression of EGFP under the chick beta-actin promoter. We find that there is full overlap between HNK-1 expression and GFP<sup>+</sup> migrating neural crest cells (Figure 3A, 3A'). In contrast, HNK-1 staining shows an absence of ephrin-A5<sup>+</sup>/GFP<sup>+</sup> NCC in BA3 with the lateral domain of HNK-1 staining devoid of ephrin-A5<sup>+</sup>/GFP<sup>+</sup> neural crest cells (Figure 3B, 3B' asterisk). Ephrin-A5<sup>+</sup>/GFP<sup>+</sup> neural crest cells are able to fully populate BA4, covering a domain comparable to control (Figure 3A, A', 3B, B', arrowhead). In addition, we checked for proper branchial arch development by staining with a pan-Dlx antibody and found that there was no noticeable difference between embryos electroporated with *pmes*-ephrin-A5 or *pca*-EGFP (Figure 3C, 3D), ruling out the possibility that BA3 is developing incorrectly and indirectly affecting the migration of ephrin-A5<sup>+</sup>/GFP<sup>+</sup> neural crest cells. Therefore, ectopic expression of ephrin-A5 specifically targets neural crest cells that normally populate BA3.

#### *r6 NCC do not migrate to BA4*

Neural crest cells that normally contribute to BA3 are derived from r5, r6, and r7, with the majority coming from r6 (Le Douarin and Kalcheim, 1999). Neural crest cells from r6 migrate primarily to BA3, with a small minority to BA4. Ablation of r5 and r6 after the neural tube loses the capacity to regenerate additional neural crest cells leads to a rerouting of neighboring neural crest cells,

which compensate for their absent neighbors and form normal craniofacial structures (Saldivar et al., 1997). The absence of neural crest cells within BA3 could potentially be due to a redirection of the r6 neural crest cells to BA4. To test this possibility, we focally labeled r6 premigratory neural crest cells with lipophilic vital dye Dil immediately following electroporation. In control embryos electroporated with *pca*-EGFP, focally labeled r6 neural crest cells can be seen along the migratory pathway to BA3 (Figure 4A', arrow) and predominantly populate BA3 (Figure 4A', arrowhead), with a small minority that end up in BA4. In embryos electroporated with *pmes*-ephrin-A5, we did not observe any r6 neural crest cells in BA3, despite the presence of Dil positive, unelectroporated, r6 neural crest cells in BA3 (Figure 4B, 4B' arrowhead). We did find ephrin-A5+/GFP+ neural crest cells from r6 along the migratory pathway to BA3 (Figure 4B', arrow) as well as in the region between BA3 and BA4. Surprisingly, we did not observe any r6 ephrin-A5+/GFP+ neural crest cells in BA4. Our results show that absence of ephrin-A5+/GFP+ neural crest cells from BA3 is unlikely to be due to a redirection of r6 ephrin-A5+/GFP+ neural crest cells to BA4.

*Ectopic EphA4 expression within the neural crest leads to mismigration along the otic vesicle*

Ectopic ephrin-A5 expression has a subtle and specific effect on the neural crest cells that populate BA3. Ephrin-A5 is able to interact with members of the EphA family of receptors as well as EphB2 (Himanen et al., 2004). Since *pmes*-ephrin-A5 drives the expression of full-length ephrin-A5, the effects that we

observe could be due to a non-cell autonomous mechanism, with the ephrin-A5+/GFP+ neural crest cells responding to Ephs in the environment. To probe the effect of Eph/ephrin signaling from the point of view of a receptor, we perturbed EphA4 activity by electroporating embryos with *pca-EphA4(int)*, a construct that drives the expression of the intracellular domain of EphA4 and is fused to EGFP and tagged with a membrane-targeting sequence (Xu et al., 1995, personal communication). Increased EphA4 activity causes neural crest cells to mis-migrate around the otic vesicle and fill in the region between BA2 and BA3 (compare Figure 5A with 5B, asterisk). Misexpression of *pca-EphA4(kd)*, the kinase-dead version of *pca-EphA4(int)*, results in fewer migrating neural crest cells, which also mis-migrate along the otic vesicle (Figure 5C, arrows). EphA4 activity, therefore, seems to have a more global effect on cranial neural crest migration than ectopic expression of ephrin-A5.

#### *Extensive migration observed in perturbed embryos*

Neural crest cells dynamically extend and retract filopodial extensions as they migrate (Kulesa et al., 2005, personal observations). In order to understand how changes in the levels of ephrin-A5 and EphA4 activity in cranial neural crest cells might change their migratory behavior, we conducted time-lapse analysis of GFP+, ephrin-A5+/GFP+, and EphA4(int)+/GFP+ cranial neural crest cells as they migrate within the intact embryo. In embryos electroporated with *pmes-ephrin-A5* or *pca-EphA4(int)*, we observe similar levels of dynamic cell behaviors during migration in our time-lapse sessions. We do not see clear differences in

cell shape changes. Ephrin-A5+/GFP+ and EphA4(int)+/EGFP+ cells also migrate extensively as distinct individuals and do not seem to have increased levels of adhesion or repulsion (Figure 6A-C).

We projected and depth coded each time-lapse data set with respect to time, such that blue represents where cells are at the start of a time-lapse imaging session, and red is where the cells are at the end. In control embryos, GFP+ neural crest cells migrate extensively away from the neural tube, as do ephrin-A5+/GFP+ and EphA4(int)+/GFP+ cells (Figure 6A-C). As we have ruled out redirection of these r6 cells as a possible cause for the absence of neural crest cells from BA3 that we observed, we focused more closely on cells migrating from r6 (Figure 6A'-C'). During migration, GFP+ r6 neural crest cells migrate diagonally and posteriorly from the neural tube towards BA3 (Figure 6A'). In contrast, ephrin-A5+/GFP+ r6 neural crest cells seem to migrate in a truncated fashion (Figure 6B'). EphA4(int)+/GFP+ r6 neural crest cells, on the other hand, misdirect around the otic vesicle (Figure 6C', arrow).

We quantified some aspects of the migration to gain insights into how our ephrin-A5 perturbation affects the migration of individual cells. We conducted cell-tracking analysis specifically on the r6 subpopulation of neural crest cells and compared the values for velocity; track length (i.e., the total distance traveled by the cell); displacement (i.e., the net distance traveled); and directionality, which is a ratio of track length to displacement. If a cell changes direction often during migration, it will have a lower directionality value than a cell that migrates along a straight path. Cell-tracking analysis reveals that ephrin-A5+/GFP+ r6 neural crest

cells migrate significantly less than do control GFP+ r6 neural crest cells (Table 2), both in terms of total track length (-31%,  $p < 0.001$ ) and displacement (-42%,  $p < 0.0001$ ). In addition, ephrin-A5+/GFP+ r6 neural crest cells migrate slightly slower than their counterparts. Interestingly, the directionality values are comparable to the control, suggesting that ectopic expression of ephrin-A5 is unlikely to affect how these cells interpret extrinsic guidance cues.

*EphA4(int)+/GFP+ neural crest cells migrate erratically.*

To visualize the pathways taken by migratory neural crest cells, cell-tracking analysis was conducted using Imaris software. Cells are identified based on brightness and size, and followed from frame to frame. A few examples of the paths are shown in Figure 6 (G-I). In control embryos, post-otic, GFP+ neural crest cells can be seen migrating along a diagonal trajectory towards BA3 and BA4. The pathways are almost parallel to each other and very organized (Figure 6G). Ephrin-A5+/GFP+ neural crest cells also migrate in an ordered fashion, though the tracks are directed upwards (Figure 6H). One of the striking changes due to ectopic expression of EphA4(int) is erratic migratory behavior seen in some EphA4+/GFP+ cells. While most post-otic cells follow pathways toward their BA3 or BA4 destinations, some EphA4+/GFP+ cells actually turn around and migrate backwards towards the neural tube (Figure 6I, arrow). Erratic cell behavior is also seen in neural crest cells from the r4 stream, where one cell can be seen actively mismigrating into the r3 repulsive zone (not shown). Increased

EphA4 activity seems to affect the way in which neural crest cells react to guidance cues within the extrinsic environment.

*Cell-tracking analysis reveals different effects on migration in cells ectopically expressing ephrin-A5 or EphA4(int)*

In control embryos electroporated with *pca*-EGFP, we found that the post-otic, cranial neural crest cells traveled about 64  $\mu\text{m}$  away from the neural tube at an average speed of 59  $\mu\text{m/hr}$  (Table 1). This is comparable to previous time-lapse studies of Dil-labeled, cranial neural crest cell migration in a whole-embryo explant culture system (Kulesa and Fraser 1998). Ephrin-A5+/GFP+ neural crest cells migrate with comparable average velocity, track length, displacement, and directionality values to control GFP+ neural crest cells (Table 1). In contrast, EphA4(int)+/GFP+ neural crest cells migrate 33% faster ( $p=0.04$ ), with significantly lower directionality (- 52%,  $p=0.0008$ ) than control GFP+ neural crest cells (Table 2). As a result, the net distance that they travel is lower (- 42%,  $p=0.125$ ) than that of GFP+ cells. Slight changes in migratory pathways correspond with changes in migratory behavior, which implies that the inherent cellular machinery responsible for migration can be modulated according to guidance cues. Therefore, ectopic EphA4 activity has a greater effect on the migration of cranial neural crest cells while ectopic ephrin-A5 primarily affects the r6 subpopulation.

## ***Discussion***

The molecular cues underlying cranial neural crest migration are largely unknown. Here, we test the potential role of Eph/ephrin signaling by perturbing the levels of ephrin-A5 and EphA4 activity in migratory cranial neural crest cells. We find that ectopic expression of ephrin-A5 specifically causes the r6 subpopulation of cranial neural crest cells to cease migration prematurely, and leads to an absence of neural crest cells within BA3 (Figure 9A). Ectopic level of EphA4 activity causes neural crest cells from both the r4 and r6 streams to migrate aberrantly along the otic vesicle (Figure 9B). In addition, we show that these cells often migrate faster, but with less directionality. Surprisingly, expression of a kinase-dead form of truncated EphA4 also leads to aberrant migration along the otic vesicle. Our results demonstrate that Eph/ephrin signaling likely affects several aspects of migration, and highlight how changes in migratory behavior results in changes in pathfinding.

### ***Different mechanisms for different axial levels***

Eph/ephrin signaling may have different roles during cranial neural crest migration at different axial levels. The cranial neural crest cells are differentially affected by ectopic expression of ephrin-A5. Most of the neural crest cells migrate normally despite ectopic expression of ephrin-A5, with the exception of the r6 subpopulation (Figure 9A). At the r4 level, other cues, such as ErbB4, and the physical obstacle posed by the otic vesicle, may play a larger role in guiding migration of that stream.

We find that EphA4 is expressed in regions that are potentially attractive to migrating neural crest cells, such as the r4 surface ectoderm and r6 mesenchyme (Figure 1). At the same time, it is also expressed in the otic vesicle (Figure 1D), an area that is repulsive to neural crest cells. EphA4 has the potential to mediate either attraction or repulsion during cranial neural crest migration, depending on the context of other ephrin ligands, as well as other signaling pathways now known to cross-talk with Eph/ephrin pathways (reviewed in Pasquale, 2005). Recent studies have also pointed to the involvement of Wnt3-Ryk and Dishevelled in modulating EphB-ephrinB interactions (Lee and Warchol, 2005; Schmitt et al., 2006). Metalloproteases, such as Adam10, have been shown to cleave actively bound ephrin-A5/EphA3 and act as a switch for contact-mediated repulsion (Janes et al., 2005). Our studies utilized a truncated form of EphA4 that only contains the intracellular portion and should act cell-autonomously (Figure 8B). It will be interesting to see whether bi-directional signaling or other signaling pathways are involved in mediating the effects of EphA4.

In addition, expression of the kinase-dead version of our EphA4 construct (which should act as a dominant negative), leads to similar levels of aberrant migration along the otic vesicle. We postulate that this could be due to recruitment of downstream factors. EphB6 does not contain a catalytic kinase domain, but is able to effect downstream signaling by recruitment of Src to respond to high/low levels of ephrin ligand (Matsuoka et al., 2005).

*Ephrin-A4 and EphA4 act at different steps during the migration process*

Ectopic ephrin-A5 specifically leads to truncated migration by the r6 neural crest cells. The cells migrate with the same directionality as the control, suggesting that guidance, per se, is not affected. Ephrin-A5 primarily interacts with EphA receptors and can bind to EphB receptors at high levels (Himeman 2004). The extent to which GPI-linked ephrin-A ligands propagate reverse signaling is not clearly understood. Together, this suggests that r6 neural crest cells do not require ephrin forward signaling for guidance during this early part of migration from the neural tube. Instead, we postulate that ephrin-A5 plays a role in cessation of migration in the r6 subpopulation.

In *Xenopus*, Eph/ephrin signaling prevents mixing of neighboring streams of cranial neural crest cells, which first migrate out from the neural tube as a uniform wave and then segregate into separate streams. In chick, the r2 and r4 streams are separated by a crest-free zone adjacent to r3. The r4 and r6 streams are separated by the otic vesicle. Neural crest cells within the r6 stream segregate between BA3 and BA4 and are most similar to the migration taken by *Xenopus* cranial neural crest. Surprisingly, we did not detect aberrant mixing of BA3 and BA4 neural crest cells. Ectopic levels of EphA4 activity causes the general population of cranial neural crest cells to migrate erratically—that is, the cells often display drastic pathfinding errors such as migrating back to the neural tube instead of towards the branchial arch, migrating into the r3 repulsive zone, or migrating around the otic vesicle. Our findings do not rule out Eph/ephrin involvement in the segregation of adjacent neural crest streams. However, our

data suggest that EphA4 likely has a more direct role in guidance of neural crest cells.

### *Concentration versus migration*

Concentration of Eph/ephrin molecules at the cell surface is believed to be the primary mechanism to fine-tune guidance of retinotectal axons and migrating cells. The *pca-EphA4(int)* construct drives the expression of EphA4(int) directly fused with EGFP, so there is a direct relationship between pixel intensity and EphA4(int) concentration. The relationship is indirect with *pmes-ephrin-A5*, which drives the independent expression of EGFP through an IRES. However, brightness should still be proportional to mRNA level, and therefore protein level, and provide information about the relative concentration of ephrin-A5 between different cells. To examine whether pixel intensity was correlated with the spatial distribution of the migratory neural crest cells from the neural tube, we created profile plots of the pixel intensities across the neural tube and post-otic, migratory neural crest cells, every 2.5 hours during time-lapse sessions. In control embryos, two peaks are quickly formed. One, which stays stationary, is the neural tube (Figure 7A, asterisk). The second is that of migratory neural crest cells (Figure 7A, arrow), which moves laterally as migration progresses. In embryos electroporated with *pmes-ephrin-A5* and *pca-EphA4(int)*, the secondary peaks remain small (Figure 7B, C). If higher levels of EphA4(int) or ephrin-A5 lead cells to cease migration at a certain point, this should give rise to a

stationary peak, and be observable in our time-lapse data. There does not appear to be a specific spatial distribution of cells based on level of expression.

*Changes in pathways reflect changes in migratory behavior*

By following cellular migration in real-time, we are able to demonstrate how pathfinding defects and changes in migratory behavior are related. In our ephrin-A5 experiments, r6 cells, which normally populate BA3, instead cease migration close to the neural tube (about 42% closer than normal,  $p < 0.0001$ ). Interestingly, ephrin-A5+/GFP+ r6 neural crest cells do not change direction any more or less than normal r6 neural crest cells, suggesting that they are likely able to read the same extrinsic guidance cues as do their counterparts. Ectopic levels of EphA4 activity cause neural crest cells to follow more disorganized paths (Figure 9B). In addition to this, these cells show a 52% reduction in directionality, which suggests that these neural crest cells change direction much more often than normal. EphA4(int)+/GFP+ cells also migrate 33% faster. These changes in migratory behavior reflect the disorganized pathways captured in our time-lapse sessions. Lastly, ectopic ephrin-A5 expression does not seem to change cell morphology, whereas ectopic EphA4 activity tends to cause cells to adopt a round shape. Interestingly, many EphA4(int)+/GFP+ cells that express less of the construct and are dimmer have normal cellular morphology.

Our study has found a direct link between the migratory behavior and pathfinding of cranial neural crest cells. Future studies to elucidate which specific Eph/ephrin family members are involved will be crucial to our understanding of

cranial neural crest cell migration. In addition, understanding how the internal cellular machinery changes to mediate migration will be useful in understanding how pathfinding occurs in other types of migratory cells.

### ***Acknowledgements***

We thank C. Krull for providing the pmes-EphrinA5 construct, R. Krumlauf for providing the pca-GFP construct, and Q. Xu and D. Wilkinson for providing the EphA4 constructs. We thank R. Baker and P. Antin for providing probes to EphA4 and EphrinA5, among others. We thank E. Pasquale for providing the EphA4 antibody. C. Lu would like to thank P. Kulesa for his expertise, and members of the Fraser and Bronner-Fraser labs for helpful discussions.

### ***References***

**Baker, R. K. and Antin, P. B.** (2003). Ephs and ephrins during early stages of chick embryogenesis. *Dev Dyn* **228**, 128-42.

**Barembaum, M. and Bronner-Fraser, M.** (2005). Early steps in neural crest specification. *Semin Cell Dev Biol* **16**, 642-6.

**Basch, M. L., Garcia-Castro, M. I. and Bronner-Fraser, M.** (2004). Molecular mechanisms of neural crest induction. *Birth Defects Res C Embryo Today* **72**, 109-23.

**Becker, N., Gilardi-Hebenstreit, P., Seitanidou, T., Wilkinson, D. and Charnay, P.** (1995). Characterisation of the Sek-1 receptor tyrosine kinase. *FEBS Lett* **368**, 353-7.

**Bronner-Fraser, M.** (1986). Analysis of the early stages of trunk neural crest migration in avian embryos using monoclonal antibody HNK-1. *Dev Biol* **115**, 44-55.

**Cornell, R. A. and Eisen, J. S.** (2005). Notch in the pathway: the roles of Notch signaling in neural crest development. *Semin Cell Dev Biol* **16**, 663-72.

**Davy, A., Aubin, J. and Soriano, P.** (2004). Ephrin-B1 forward and reverse signaling are required during mouse development. *Genes Dev* **18**, 572-83.

**Davy, A. and Soriano, P.** (2005). Ephrin signaling in vivo: look both ways. *Dev Dyn* **232**, 1-10.

**Eberhart, J., Swartz, M. E., Koblar, S. A., Pasquale, E. B. and Krull, C. E.** (2002). EphA4 constitutes a population-specific guidance cue for motor neurons. *Dev Biol* **247**, 89-101.

**Ellies, D. L., Tucker, A. S. and Lumsden, A.** (2002). Apoptosis of premigratory neural crest cells in rhombomeres 3 and 5: consequences for patterning of the branchial region. *Dev Biol* **251**, 118-28.

**Farlie, P., Kerr, R., Thomas, P., Symes, T., Minichiello, J., Hern, C. and Newgreen, D.** (1999). A paraxial exclusion zone creates patterned cranial neural crest cell outgrowth adjacent to rhombomeres 3 and 5. *Dev Biol* **213**, 70-84.

**Gammill, L. S. and Bronner-Fraser, M.** (2002). Genomic analysis of neural crest induction. *Development* **129**, 5731-41.

**Gammill, L. S., Gonzalez, C., Gu, C. and Bronner-Fraser, M.** (2006). Guidance of trunk neural crest migration requires neuropilin 2/semaphorin 3F signaling. *Development* **133**, 99-106.

**Golding, J. P., Sobieszczuk, D., Dixon, M., Coles, E., Christiansen, J., Wilkinson, D. and Gassmann, M.** (2004). Roles of ErbB4, rhombomere-

specific, and rhombomere-independent cues in maintaining neural crest free zones in the embryonic head. *Dev Biol* **266**, 361-72.

**Golding, J. P., Trainor, P., Krumlauf, R. and Gassmann, M.** (2000). Defects in pathfinding by cranial neural crest cells in mice lacking the neuregulin receptor ErbB4. *Nat Cell Biol* **2**, 103-9.

**Guthrie, S.** (1996). Patterning the hindbrain. *Curr Opin Neurobiol* **6**, 41-8.

**Hamburger, V. and Hamilton, H. L.** (1951). A series of normal stages in the development of the chick embryo. *J Morphology* **88**, 49-92.

**Helbling, P. M., Tran, C. T. and Brandli, A. W.** (1998). Requirement for EphA receptor signaling in the segregation of *Xenopus* third and fourth arch neural crest cells. *Mech Dev* **78**, 63-79.

**Himanen, J. P., Chumley, M. J., Lackmann, M., Li, C., Barton, W. A., Jeffrey, P. D., Vearing, C., Geleick, D., Feldheim, D. A., Boyd, A. W. et al.** (2004). Repelling class discrimination: ephrin-A5 binds to and activates EphB2 receptor signaling. *Nat Neurosci* **7**, 501-9.

**Hunt, P., Whiting, J., Muchamore, I., Marshall, H. and Krumlauf, R.** (1991). Homeobox genes and models for patterning the hindbrain and branchial arches. *Dev Suppl* **1**, 187-96.

**Itasaki, N., Bel-Vialar, S. and Krumlauf, R.** (1999). 'Shocking' developments in chick embryology: electroporation and in ovo gene expression. *Nat Cell Biol* **1**, E203-E207.

**Janes, P. W., Saha, N., Barton, W. A., Kolev, M. V., Wimmer-Kleikamp, S. H., Nievergall, E., Blobel, C. P., Himanen, J. P., Lackmann, M. and Nikolov, D.**

- B.** (2005). Adam meets Eph: an ADAM substrate recognition module acts as a molecular switch for ephrin cleavage in trans. *Cell* **123**, 291-304.
- Kontges, G. and Lumsden, A.** (1996). Rhombencephalic neural crest segmentation is preserved throughout craniofacial ontogeny. *Development* **122**, 3229-3242.
- Krull, C. E.** (1998). Inhibitory interactions in the patterning of trunk neural crest migration. *Ann N Y Acad Sci* **857**, 13-22.
- Krull, C. E., Lansford, R., Gale, N. W., Collazo, A., Marcelle, C., Yancopoulos, G. D., Fraser, S. E. and Bronner-Fraser, M.** (1997). Interactions of Eph-related receptors and ligands confer rostrocaudal pattern to trunk neural crest migration. *Curr Biol* **7**, 571-80.
- Krull, C. E. and Kulesa, P. M.** (1998). Embryonic explant and slice preparations for studies of cell migration and axon guidance. *Curr Top Dev Biol* **36**, 145-59.
- Kulesa, P., Bronner-Fraser, M. and Fraser, S.** (2000). In ovo time-lapse analysis after dorsal neural tube ablation shows rerouting of chick hindbrain neural crest. *Development* **127**, 2843-52.
- Kulesa, P. and Fraser, S.** (1998a). Neural crest cell dynamics revealed by time-lapse video microscopy of whole embryo chick explant cultures. *Dev Biol* **204**, 327-344.
- Kulesa, P. M. and Fraser, S. E.** (1998b). Segmentation of the vertebrate hindbrain: a time-lapse analysis. *Int J Dev Biol* **42**, 385-92.
- Kulesa, P. M. and Fraser, S. E.** (1999). Confocal imaging of living cells in intact embryos. *Methods Mol Biol* **122**, 205-22.

- Kulesa, P. M. and Fraser, S. E.** (2000). In ovo time-lapse analysis of chick hindbrain neural crest cell migration shows cell interactions during migration to the branchial arches. *Development* **127**, 1161-72.
- Kulesa, P. M., Lu, C. C. and Fraser, S. E.** (2005). Time-lapse analysis reveals a series of events by which cranial neural crest cells reroute around physical barriers. *Brain Behav Evol* **66**, 255-65.
- Le Douarin, N. and Kalcheim, C.** (1999). *The Neural Crest*, 2nd ed. Cambridge: Cambridge University Press.
- Lee, K. H. and Warchol, M. E.** (2005). Ephrin A2 may play a role in axon guidance during hair cell regeneration. *Laryngoscope* **115**, 1021-5.
- Lumsden, A. and Guthrie, S.** (1991). Alternating patterns of cell surface properties and neural crest cell migration during segmentation of the chick hindbrain. *Development Suppl* **2**, 9-15.
- Lumsden, A. and Krumlauf, R.** (1996). Patterning the vertebrate neuraxis. *Science* **274**, 1109-15.
- Matsuoka, H., Obama, H., Kelly, M. L., Matsui, T. and Nakamoto, M.** (2005). Biphasic functions of the kinase-defective Ephb6 receptor in cell adhesion and migration. *J Biol Chem* **280**, 29355-63.
- Momose, T., Tonegawa, A., Takeuchi, J., Ogawa, H., Umesono, K. and Yasuda, K.** (1999). Efficient targeting of gene expression in chick embryos by microelectroporation. *Dev Growth Differ* **41**, 335-44.
- Morales, A. V., Barbas, J. A. and Nieto, M. A.** (2005). How to become neural crest: from segregation to delamination. *Semin Cell Dev Biol* **16**, 655-62.

- Panganiban, G., Sebring, A., Nagy, L. and Carroll, S.** (1995). The development of crustacean limbs and the evolution of arthropods. *Science* **270**, 1363-6.
- Pasquale, E. B.** (2005). Eph receptor signalling casts a wide net on cell behaviour. *Nat Rev Mol Cell Biol* **6**, 462-75.
- Raible, D. W. and Ragland, J. W.** (2005). Reiterated Wnt and BMP signals in neural crest development. *Semin Cell Dev Biol* **16**, 673-82.
- Rasband, W. S. and Bright, D. S.** (1995). NIH Image: A public domain image processing program for the Macintosh. *Microbeam Analysis* **4**, 137-149.
- Rickmann, M., Fawcett, J. W. and Keynes, R. J.** (1985). The migration of neural crest cells and the growth of motor axons through the rostral half of the chick somite. *J Embryol Exp Morphol* **90**, 437-55.
- Sadaghiani, B. and Thiebaud, C. H.** (1987). Neural crest development in the *Xenopus laevis* embryo, studied by interspecific transplantation and scanning electron microscopy. *Dev Biol* **124**, 91-110.
- Saldivar, J., Sechrist, J., Krull, C., Ruffins, S. and Bronner-Fraser, M.** (1997). Dorsal hindbrain ablation results in rerouting of neural crest migration and changes in gene expression, but normal hyoid development. *Development* **124**, 2729-2739.
- Schmitt, A. M., Shi, J., Wolf, A. M., Lu, C. C., King, L. A. and Zou, Y.** (2006). Wnt-Ryk signalling mediates medial-lateral retinotectal topographic mapping. *Nature* **439**, 31-7.

- Sechrist, J., Serbedzija, G. N., Scherson, T., Fraser, S. E. and Bronner-Fraser, M.** (1993). Segmental migration of the hindbrain neural crest does not arise from its segmental generation. *Development* **118**, 691-703.
- Serbedzija, G. N., Bronner-Fraser, M. and Fraser, S. E.** (1992). Vital dye analysis of cranial neural crest cell migration in the mouse embryo. *Development* **116**, 297-307.
- Serbedzija, G. N., Fraser, S. E. and Bronner-Fraser, M.** (1990). Pathways of trunk neural crest cell migration in the mouse embryo as revealed by vital dye labelling. *development* **108**, 605-12.
- Smith, A., Robinson, V., Patel, K. and Wilkinson, D.** (1997). The EphA4 and EphB1 receptor tyrosine kinases and ephrin-B2 ligand regulate targeted migration of branchial neural crest cells. *Curr Biol* **7**, 561-570.
- Soans, C., Holash, J. A., Pavlova, Y. and Pasquale, E. B.** (1996). Developmental expression and distinctive tyrosine phosphorylation of the Eph-related receptor tyrosine kinase Cek9. *J Cell Biol* **135**, 781-95.
- Steventon, B., Carmona-Fontaine, C. and Mayor, R.** (2005). Genetic network during neural crest induction: from cell specification to cell survival. *Semin Cell Dev Biol* **16**, 647-54.
- Swartz, M. E., Eberhart, J., Pasquale, E. B. and Krull, C. E.** (2001). EphA4/ephrin-A5 interactions in muscle precursor cell migration in the avian forelimb. *Development* **128**, 4669-80.

- Teddy, J. M. and Kulesa, P. M.** (2004). In vivo evidence for short- and long-range cell communication in cranial neural crest cells. *Development* **131**, 6141-51.
- Thévenaz, P., Ruttimann, U. E. and Unser, M.** (1998). A pyramid approach to subpixel registration based on intensity. *IEEE Transactions on Image Processing* **7**, 27-41.
- Trainor, P. and Krumlauf, R.** (2000). Plasticity in mouse neural crest cells reveals a new patterning role for cranial mesoderm. *Nature Cell Biology* **2**, 96-102.
- Trainor, P. A., Sobieszczuk, D., Wilkinson, D. and Krumlauf, R.** (2002). Signalling between the hindbrain and paraxial tissues dictates neural crest migration pathways. *Development* **129**, 433-42.
- Vaage, S.** (1969). The segmentation of the primitive neural tube in chick embryos (*Gallus domesticus*). A morphological, histochemical and autoradiographical investigation. *Ergeb Anat Entwicklungsgesch* **41**, 3-87.
- Wang, H. U. and Anderson, D. J.** (1997). Eph family transmembrane ligands can mediate repulsive guidance of trunk neural crest migration and motor axon outgrowth. *Neuron* **18**, 383-96.
- Wilkinson, D.** (1992). In *Situ Hybridization: A Practical Approach*. Oxford: IRL Press.
- Wilkinson, D. G.** (2001). Multiple roles of EPH receptors and ephrins in neural development. *Nat Rev Neurosci* **2**, 155-64.

**Xu, Q., Alldus, G., Holder, N. and Wilkinson, D. G.** (1995). Expression of truncated Sek-1 receptor tyrosine kinase disrupts the segmental restriction of gene expression in the *Xenopus* and zebrafish hindbrain. *Development* **121**, 4005-16.

**Xu, Q., Mellitzer, G. and Wilkinson, D. G.** (2000). Roles of Eph receptors and ephrins in segmental patterning. *Philos Trans R Soc Lond B Biol Sci* **355**, 993-1002.

**Figures**

*Figure 3.1: Differential expression of EphA4 and ephrin-A5 within the cranial region of an HH12 embryo.*

Whole mount in situ hybridization of EphA4 (A) and ephrin-A5 (F) with sections from r3, r4, r5, and r6. Sections are indicated with lines. EphA4 is expressed in the (B) r3 neural tube, (C) r4 surface ectoderm (arrowhead), (D) otic vesicle, and (E) r6 mesenchyme (arrow indicates surface ectoderm, with staining underneath this layer of tissue). Ephrin-A5 is expressed within the neural tube, (H) r4 mesenchyme, and (J) r6 mesenchyme (arrow). Scalebars, 100  $\mu$ m.

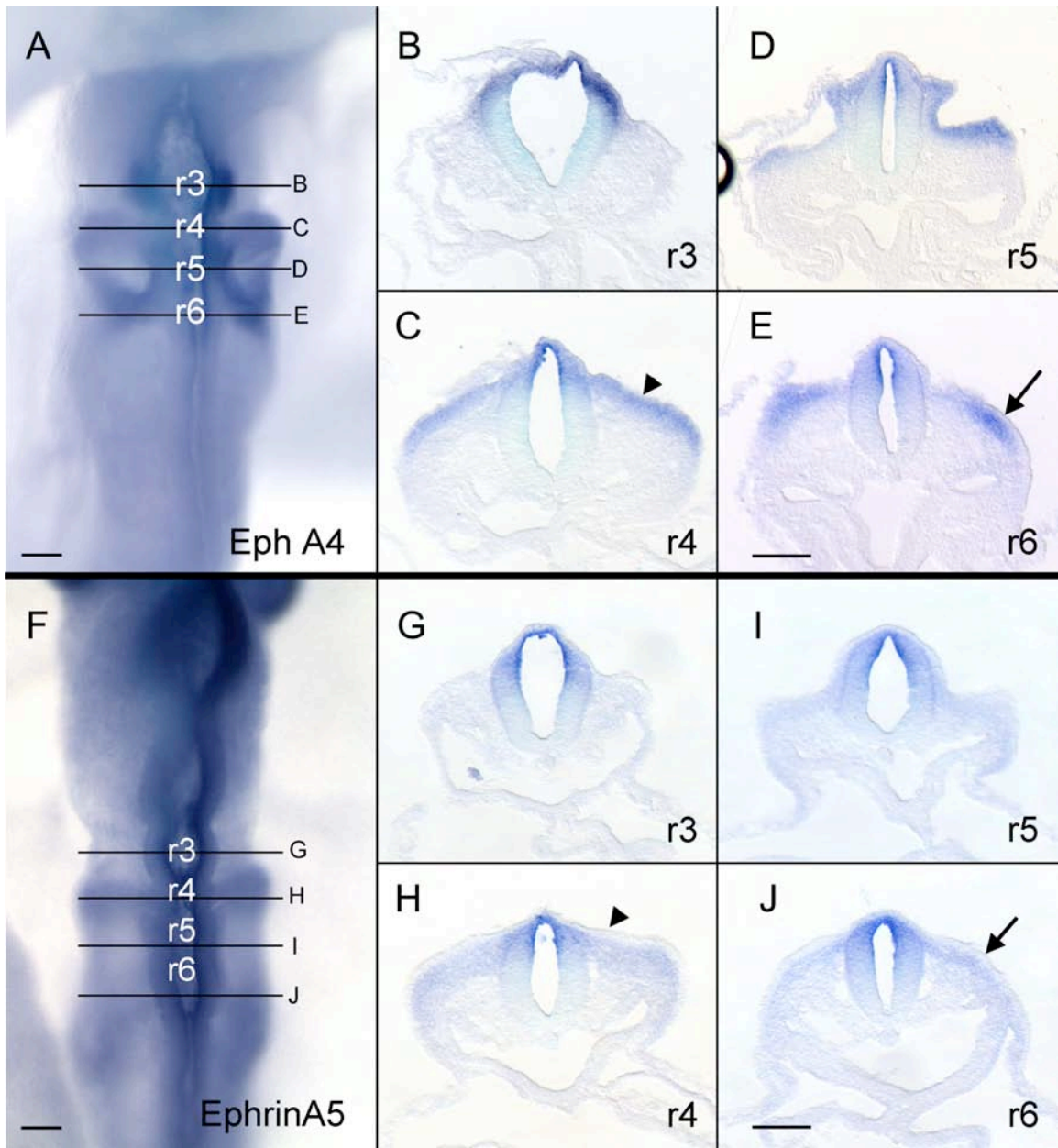


*Figure 3.2: Ectopic ephrin-A5 expression leads to fewer NCCs in BA3 initially*

Embryos were electroporated with pmes-ephrin-A5 to examine the effects of ectopic ephrin-A5 expression in neural crest cells. A'-C' are GFP-only close-ups of the boxed region in A-C. (A, A') At HH10+, or 8 hrs after electroporation, few cells are seen at the r6 level (asterisk) while there is extensive migration at other levels. (B, B') At HH12 there is a continued lack of neural crest cells in BA3 (asterisk). (C, C') By HH12 or 31 hours after electroporation there is even distribution of neural crest cells within BA3, which could be due to later migration or cell proliferation. OV, otic vesicle, BA, branchial arch.

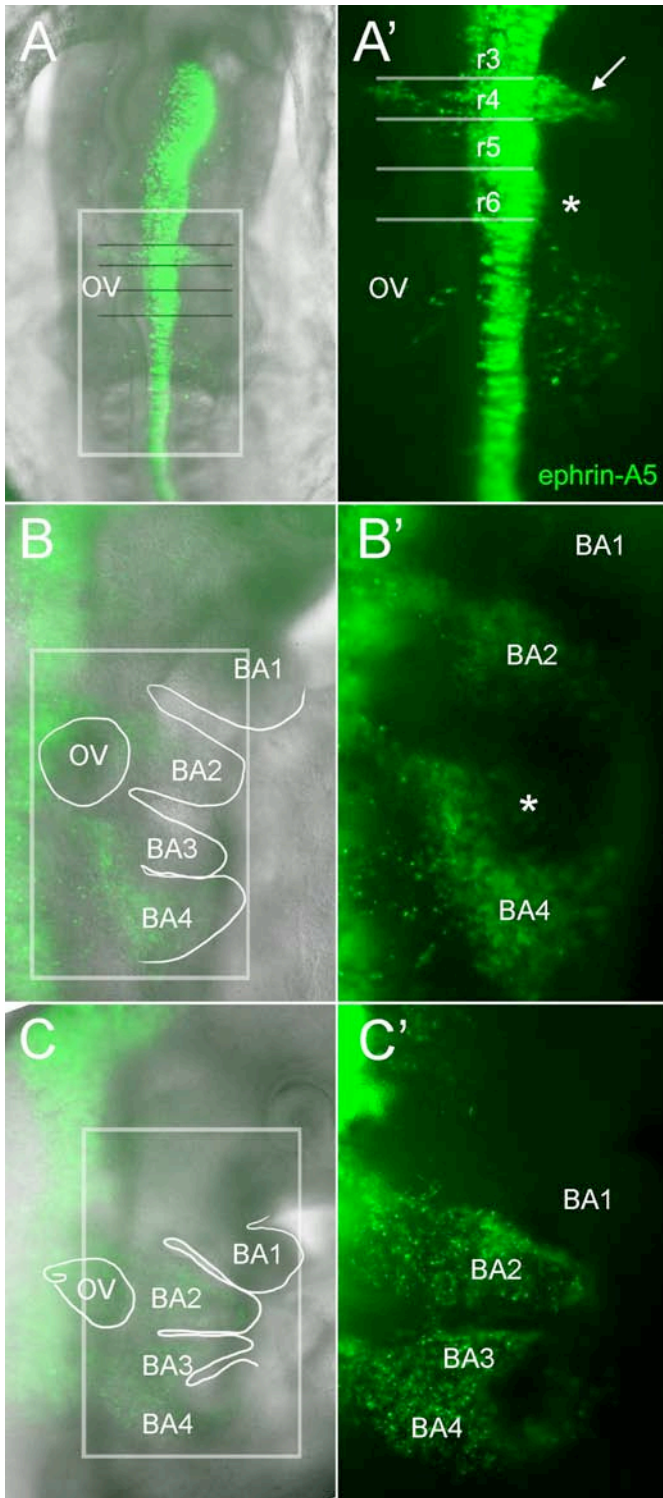


*Figure 3.3: Neural crest cells ectopically expressing ephrin-A5 do not migrate to BA3*

Embryos were electroporated with control *pca*-GFP (A, A', C) or *pmes-ephrin-A5* (B, B', D) constructs to examine the migration of neural crest cells as compared with HNK-1 staining (A,B) or pan-Dlx antibody staining (C,D). In control embryos, GFP+ cells fully overlap with HNK-1 staining (A) and populate BA3 (A', asterisk), and BA4 (A', arrowhead). In comparison, there is an absence of ephrin-A5+ NCCs in BA3 (B, B', asterisk) while BA4 seems normal (B', arrowhead). Pan-Dlx antibody staining shows normal staining in the branchial arches in embryos electroporated with *pmes-ephrin-A5* (D). OV, otic vesicle. BA, branchial arch.

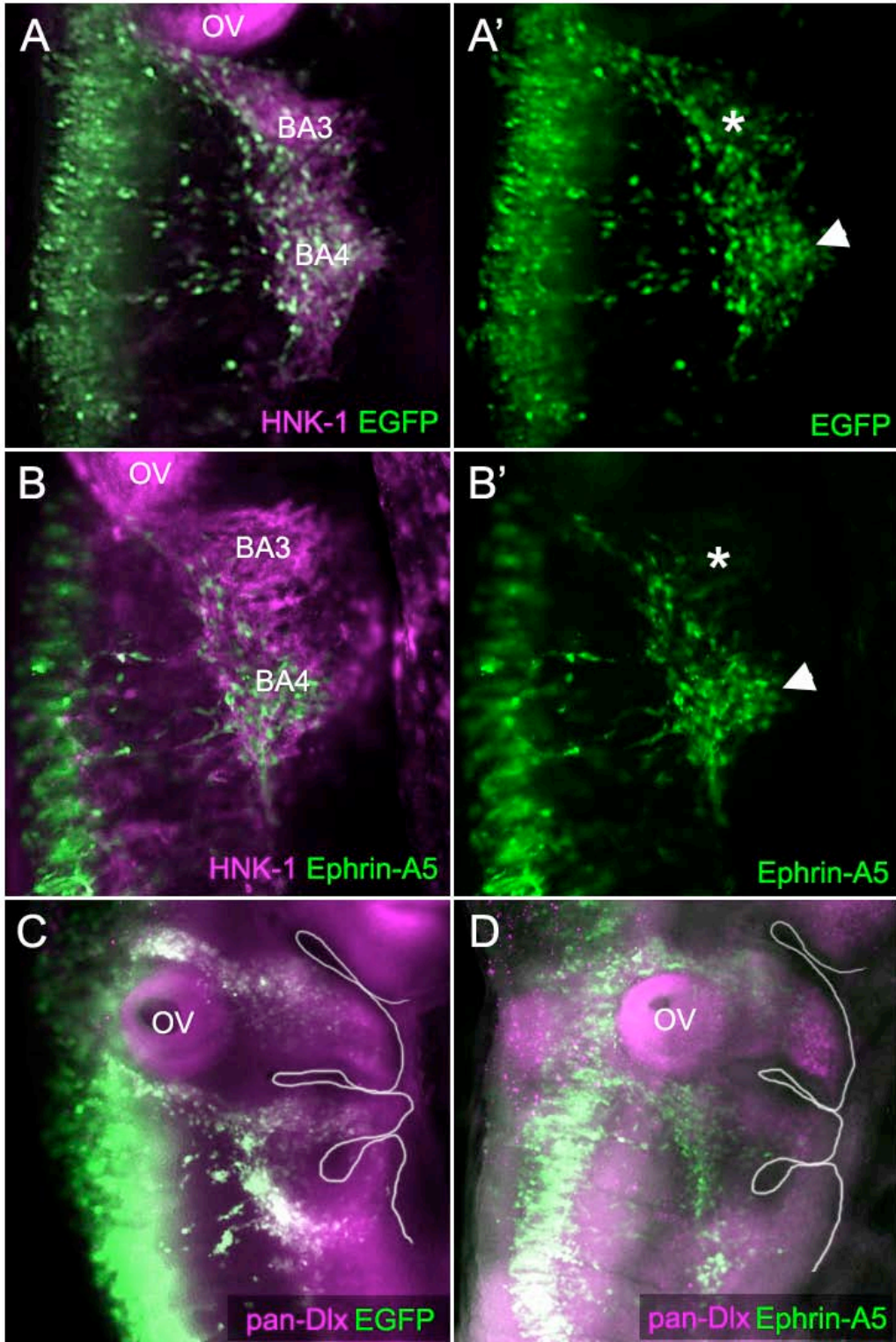


*Figure 3.4: Ephrin-A5+ r6 NCCs do not migrate to BA4*

To examine whether the r6 subpopulation of neural crest cells are being redirected to BA4 in embryos electroporated with pmes-ephrin-A5, we focally injected Dil into r6 shortly after electroporation (see inset in A', B'). In *pca*-GFP electroporated embryos (A, A'), focally labeled r6 neural crest cells migrate to BA3 (A', arrowhead), with a minority migrating to BA4. In contrast, a few ephrin-A5+ NCCs are seen migrating to BA3 (B' arrow), but only r6 neural crest cells not expressing ephrin-A5 (labeled with focally injected Dil) are able to migrate to BA3 (B', arrowhead). OV, otic vesicle. E, eye. BA, branchial arch.

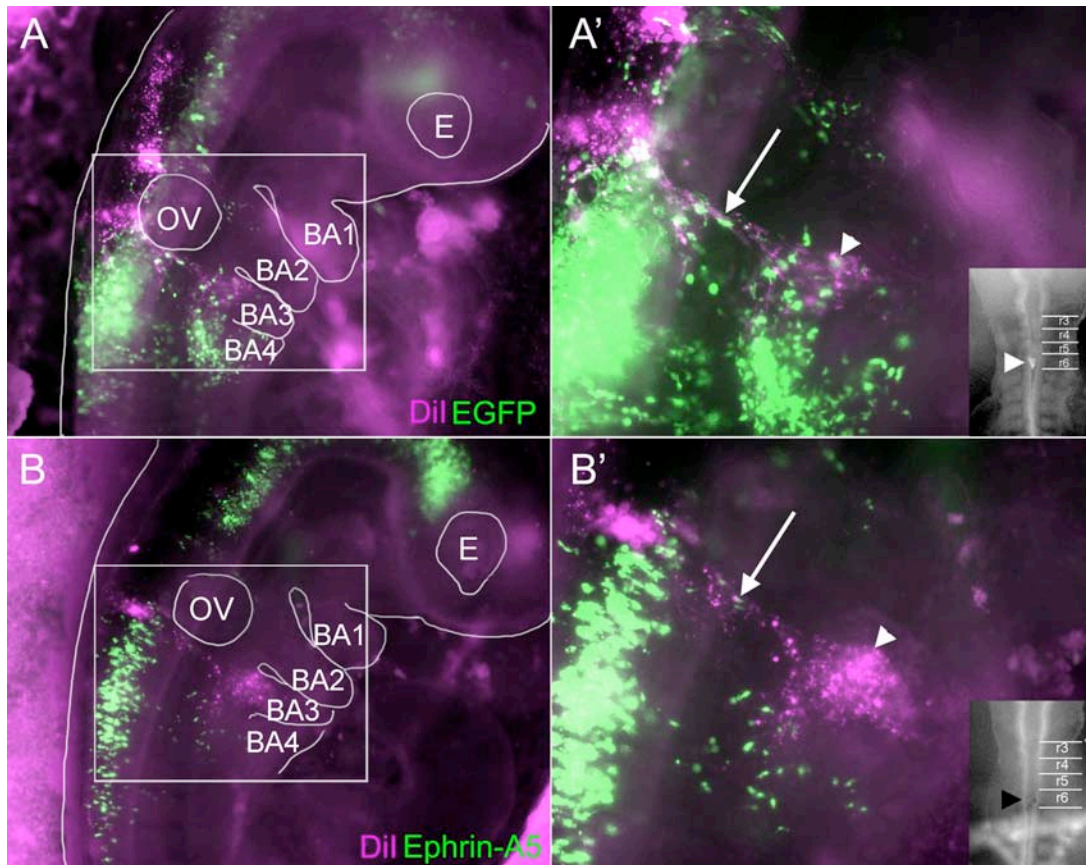


*Figure 3.5: EphA4(int) and EphA4(kd) causes mismigration along the otic vesicle*

Embryos were electroporated with *pca*-GFP as the control (A), *pca*-EphA4(int) for ectopic levels of EphA4 activity (B), and *pca*-EphA4(kd), the kinase-dead version of EphA4(int), thought to act as a dominant negative (C). Normally, there is a crest-free zone separating cells from BA2 and BA3(asterisk, A). Mismigration of neural crest cells along the otic vesicle is seen with *pca*-EphA4(int) (asterisk, B) and *pca*-EphA4(kd) (arrows, C). *pca*-EphA4(kd) also decreases the overall number of migratory neural crest cells. OV, otic vesicle. Scalebar is 200  $\mu$ m.

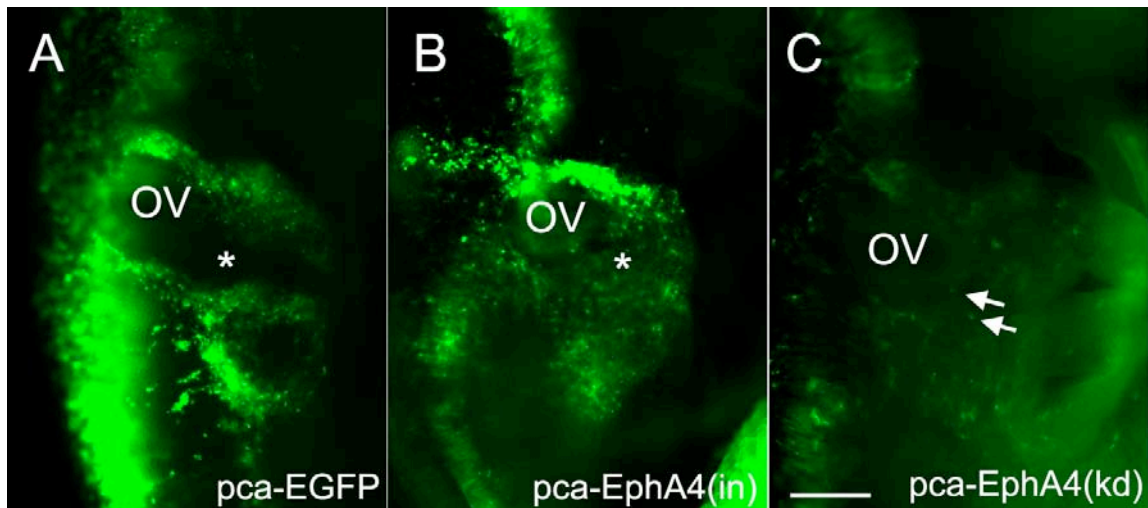


*Figure 3.6: Cell morphology, temporal distribution, and cell-tracking*

Extensive migration was observed in control embryos electroporated with *pca*-GFP, *pmes-ephrin-A5*, and *pca-EphA4(int)*. Dynamic time-lapse data show extensive filopodial and diverse cell morphologies in GFP+ (A) and *ephrin-A5+/GFP+* (B) neural crest cells. However, *EphA4(int)+* neural crest cells often displayed rounded cells (C) in addition to cells with normal morphology. Representative time-lapse data sets were projected and color-coded over time using the LSM software depth-code feature such that blue indicates where the cells are at the start and red indicates where the cells are at the end of the time-lapse. Control (D, D'), *pmes-ephrin-A5* (E, E'), and *pca-EphA4(int)* (F, F'). Close-up of the r6 region (A'-C') shows shortened tracks in r6 *ephrin-A5+/GFP+* cells (E') and mismigration along the otic vesicle by *EphA4(int)+/GFP+* cells (arrow, F'). A closer look at the migratory routes shows organized, arrayed pathways for GFP+ (G) and *ephrin-A5+/GFP+* (H) neural crest cells. *EphA4(int)+/GFP+* neural crest cells follow disorganized pathways (I). In each session, a few cells were observed migrating backwards (I, arrow) or into the r3 repulsive territory (not shown). OV, otic vesicle. Scalebar is 50  $\mu$ m for A-C, 100  $\mu$ m for D-F.

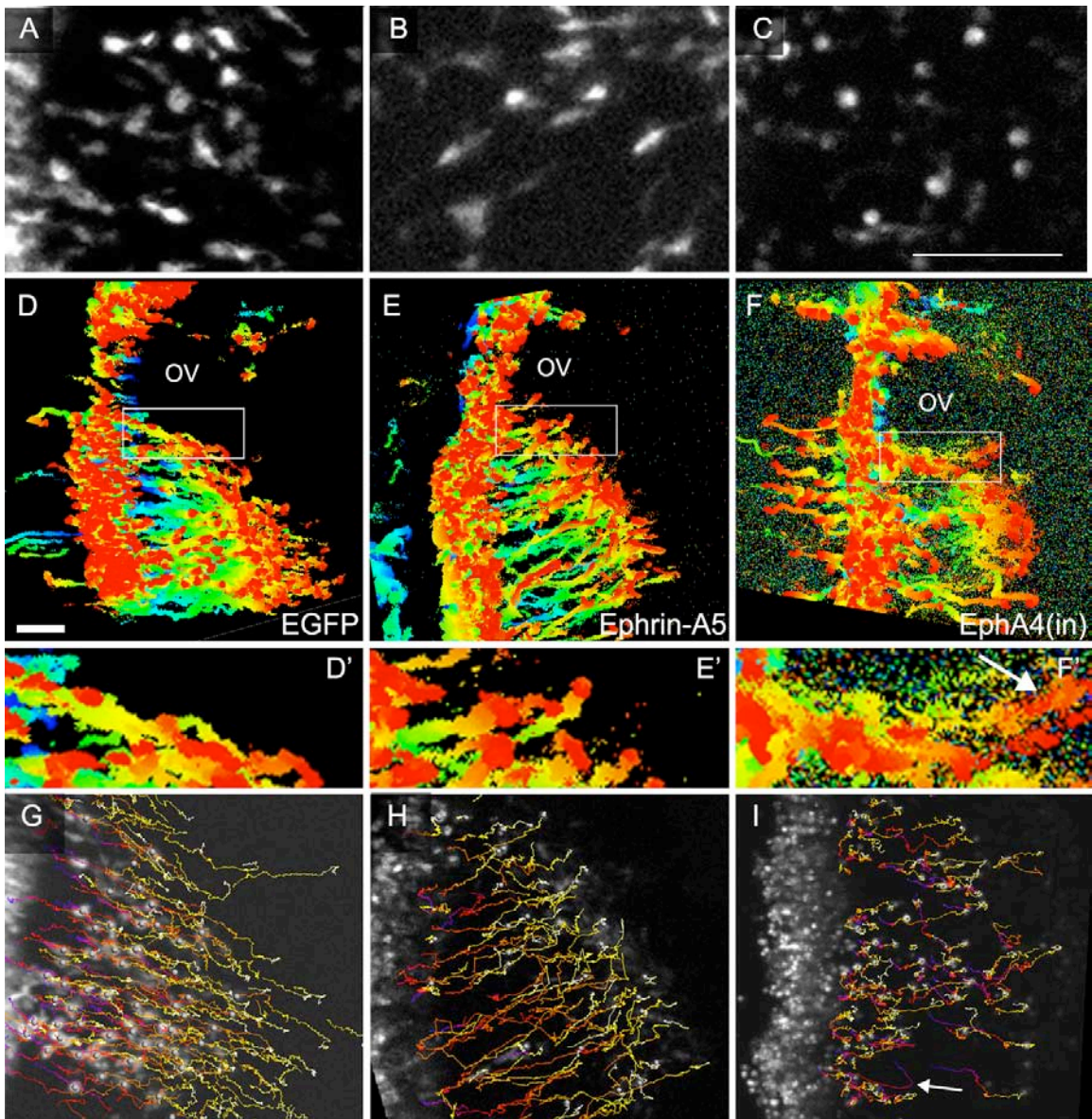


*Figure 3.7: Eph/ephrin concentration and migration*

Eph/ephrin-directed migration is believed to be dependent on migration. Since labeling by electroporation tends to be mosaic, we looked at the pixel intensity profiles of the post-otic neural crest cells every 1.5 hrs to infer the concentration of ephrin-A5 and EphA4(int). Each time-lapse was first projected across time using a standard deviation formula to identify changes in intensity over time (A-C) as an overview of cell intensities and migration in each data set. In control embryos electroporated with *pca*-GFP (below A) we see two peaks in the profile. One (asterisk) is from labeled neural tube cells and the other (arrow) is from migratory neural crest cells. In embryos electroporated with ephrin-A5 (B), the neural tube peak remains at the right (asterisk) with smaller peaks appearing over time due to migratory ephrin-A5+/GFP+ neural crest cells. In EphA4(int) profiles, the second peak remains small as well. If the concentration of Eph/ephrin determined the stopping point of the migratory neural crest cell, one might expect to see small, stationary peaks that denote where cells may have ceased migration. Instead, we see that the secondary peak tends to continue to move laterally as migration progresses. Scalebar is 100  $\mu\text{m}$ .

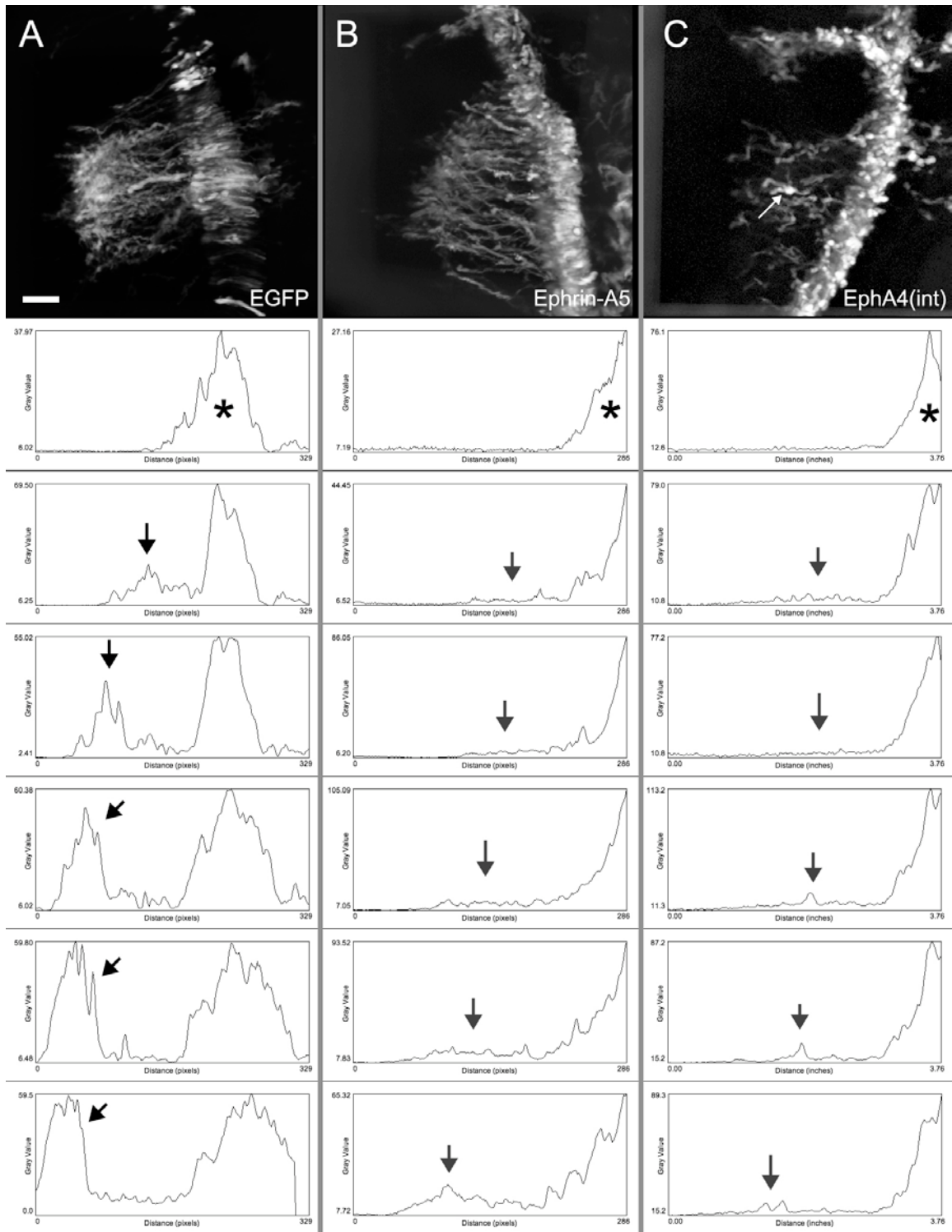


*Figure 3.8: Ectopic ephrin-A5 and EphA4 activity*

To perturb Eph/ephrin activity we overexpressed full-length ephrin-A5 (A) and a truncated intracellular version of EphA4 fused to a membrane-targeted GFP (B). Neural crest cells expressing full-length ephrin-A5 ligand could act by binding to Eph receptor expressing cells in the environment and triggering forward signaling. In addition, bi-directional signaling could also occur through associated proteins within the ephrin-A5+ cell. Ephrin-A5 can interact with EphA receptors, but can also cross-talk and interact with EphB receptors, especially when expressed at high levels (A, orange and blue domains on ephrin-A5). EphA4(int) is a truncated version that is likely to act cell-autonomously (B). In both cases, there is also the possibility that the activity of co-expressed Eph or ephrins is modulated by our constructs.

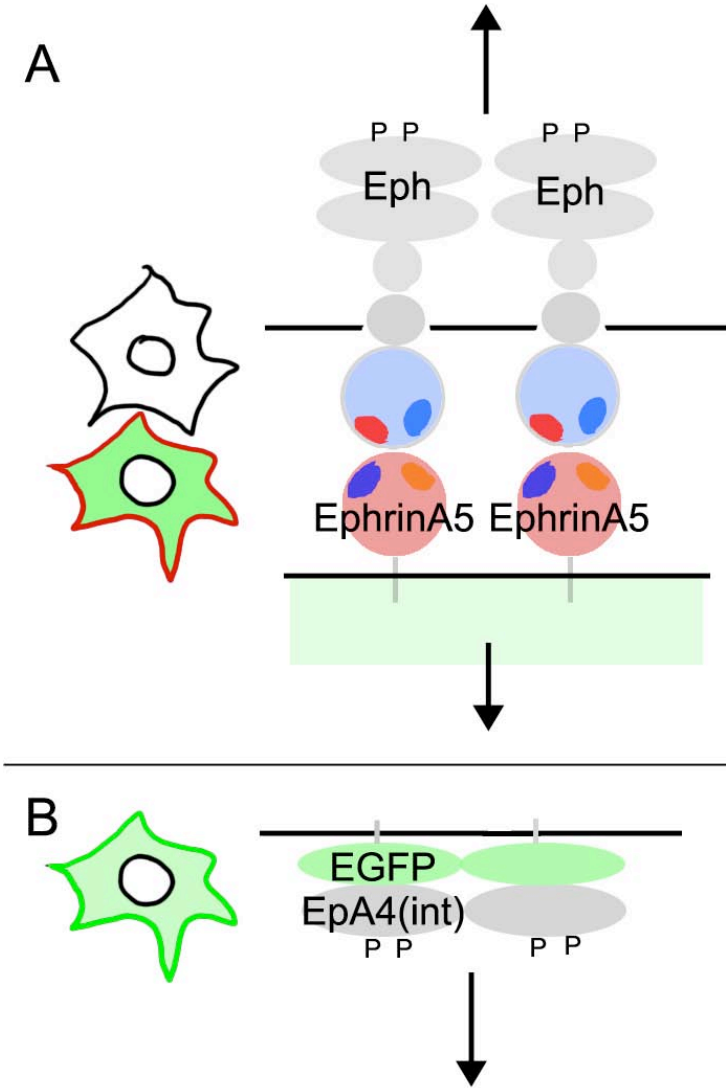


*Figure 3.9: Summary of ephrin-A5 and EphA4 perturbations*

Ectopic ephrin-A5 causes the r6 subpopulation (A, orange cells) of neural crest cells to cease migration prematurely along their normal migratory pathway (A, red arrow). However, neural crest cells in the r4 stream, more posterior hindbrain, and first few somite levels are unaffected (A, green arrows and green cells). Ectopic EphA4 activity causes neural crest cells from the r4 and r6 stream to migrate aberrantly along the otic vesicle (B, red arrows). In addition, the general migratory behavior is more erratic than normal. Cells migrate faster, but without a good sense of direction (denoted by angles in green arrows).

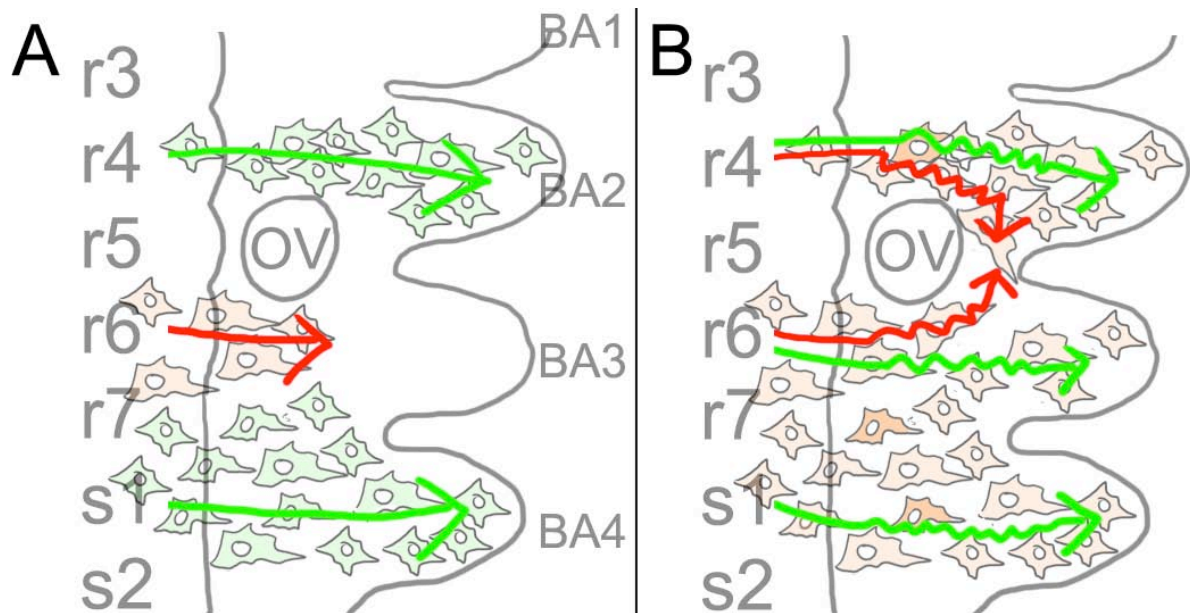


*Table 3.1: Cell tracking analysis: cranial neural crest cells*

	pca-EGFP	pmes-ephrin-A5	pca-EphA4(int)
Velocity (um/hr)	59.00	61.71 n.s.	78.49 *
SD	11.01	16.97	23.68 + 33%
SE	3.672	6.928	8.372 P=0.0422
Length (um)	194.6	178.8 n.s.	232.6 n.s.
SD	41.72	28.71	107.9
SE	13.91	11.72	38.16
Displacement (um)	63.84	57.58 n.s.	36.74 *
SD	17.97	19.74	21.41 - 42%
SE	5.991	8.057	7.569 p=0.125
Directionality	0.3554	0.3402 n.s.	0.1696 ***
SD	0.1009	0.06906	0.08016 - 52%
SE	0.03363	0.02819	0.02834 p=0.0008
# embryos	6	6	4
# tracked cells	974	789	1433

Cell-tracking analysis was carried out on 16 time-lapse sessions, each over 8 hours long. Statistical comparisons were made using an unpaired t-test.

Table 3.2: Cell tracking analysis: r6 subpopulation of cranial neural crest cells

	pca-EGFP	pmes-ephrin-A5	
Velocity (um/hr)	72.34	62.70	**
SD	19.36	23.79	- 13%
SE	1.975	3.071	p=0.0064
Length (um)	271.7	186.2	***
SD	121.1	129.7	- 31%
SE	12.36	16.75	p<0.0001
Displacement (um)	87.28	50.61	***
SD	33.54	29.25	- 42%
SE	3.423	3.776	p<0.0001
Directionality	0.3458	0.3290	n.s.
SD	0.1171	0.1736	
SE	0.01195	0.02241	
# embryos	6	5	
# tracked cells	96	60	

Cell-tracking analysis was carried out on 11 time-lapse sessions. Statistical comparisons were made using an unpaired t-test.

*Table 3.3: Rates of cell proliferation and death*

Stage		Control	Ephrin-A5	N	P value*
8 hr	Proliferation	3.23 ± 0.19	2.95 ± 0.21	57	p=0.0038
	Death	0.30 ± 0.11	1.36 ± 0.36	50	
24 hr	Proliferation	2.13 ± 0.26	3.33 ± 0.26	46	p=0.0011
	Death	0.0 ± 0.0	1.00 ± 0.63	5	
31 hr	Proliferation	3.92 ± 0.25	4.58 ± 0.26	95	p=0.0074
	Death	1.93 ± 0.34	1.33 ± 0.23	83	

\*Paired t-test of matched regions in sequential cryosections.

*Supplementary materials: cell death and cell proliferation*

To determine the levels of cell death and cell proliferation, embryos electroporated with pCAGFP or pmes-ephrin-A5 were fixed, embedded in gelatin, and cryosectioned. Individual sections were collected on three sets of slides to compare the levels of cell death, cell proliferation, and cell numbers on sequential sections. For cell death, TUNEL staining was carried out according to the manufacturer's directions (#12156792910, In situ Death Detection Kit, TMR Red, Roche Applied Science), and then followed by antibody staining. Anti-phospho-histone-3 antibody was used to detect cell proliferation. Dapi (#D1306, Molecular Probes) staining was used to label nuclei for cell counting. Stained embryos and sections were imaged on a monochrome hMR Axiocam on a Axioplan II epifluorescent upright microscope (Zeiss, Inc., Germany) equipped with the necessary filter sets (Chroma Technology, Corp., Rockingham, VT) or on an inverted Zeiss 510 confocal microscope.

Increased cell death or decreased cell proliferation rates in the premigratory ephrin-A5+/GFP+ r6 neural crest cells could also contribute to fewer cells in BA3. To examine the rates of cell death and cell proliferation in embryos electroporated on one side with pmes-ephrin-A5, we collected sequential sections and stained for phospho-histone-3 activity or TUNEL. Several regions were selected in each section and the relative amount of dying or proliferating cells was counted and compared with the corresponding regions on the unelectroporated side. We found that at 8 hours post-electroporation, there was a four-fold increase in cell death within regions of the neural tube that had been

electroporated with pmes-ephrin-A5 ( $p=0.0038$ , see Table 1). At 24 hours, we found a slight increase in both cell proliferation and cell death ( $p=0.0011$ ). Finally, at 31 hours post-electroporation, there was also a slight increase in cell proliferation ( $p=0.0074$ ) within regions electroporated with pmes-ephrin-A5. We find that ephrin-A5 has varying effects on cell death and cell proliferation. It is possible that small changes in the rates of cell death and cell proliferation could lead to the significant absence of neural crest cells in BA3 that we observe. However, we were unable to correlate these changes specifically to r6 neural crest cells. Ectopic ephrin-A5 has different effects on cell proliferation and cell death at varying stages of development.

## CHAPTER 4: Summary and Future Directions

### *Summary*

Many mechanisms are thought to shape cranial neural crest migration from the hindbrain into three streams. Intrinsic mechanisms, such as localized cell death within regions of the hindbrain and restricted exit points, could help set up a segregated pattern of migration before the neural crest cells exit the neural tube. Within the migratory neural crest cells, differential affinity between adjacent streams is thought to play a role in keeping one subpopulation of migratory neural crest cells from mixing with neighboring subpopulations. Likewise, the population model suggests migration is driven by follower cells pushing upon leaders and following leader cells. Extrinsic mechanisms such as regions of repulsive and/or attractive cues in the environment may also be involved in shaping corridors for migration.

This thesis sets out to test some of these mechanisms, paying special attention to any cell behavior changes that might occur. In Chapter 2, we first test whether the r4 stream is shaped according to the population model, where migration is directed by follower cells that push upon lead cells at the front of the stream. Lead cells are thought to lay down guidance cues for follower cells. We find that neural crest cells are able to divert away from their normal pathways to find novel paths around physical barriers. By conducting a time-lapse study of this process we discovered a few surprises. Followers do not simply push lead cells along, nor do they directly follow the paths forged by the lead cells. Instead,

lead cells often became trapped behind the barrier, and one of the follower cells goes on to forge a new path around the barrier, becoming the new leader. Our data, which show that migration continues to progress despite a decrease in the number of follower cells and the interchangeable role of leaders and followers, opposes the population model.

In the differential affinity model, subpopulations of neural crest cells preferentially associate and migrate together. Neural crest cells immediately follow behind new leaders to migrate around the barrier. In addition, neural crest cells from the r4 stream will actively migrate into repulsive r3 territory and interact with trapped r2 neural crest cells. Over time, many more neural crest cells from the r4 stream will follow, preferring to migrate over each other rather than migrating along the proper pathway. Our observations of neural crest cells following each other to form ectopic migration paths support the notion that neural crest cells are able to guide fellow neural crest cells. However, further studies will be needed to prove whether there is actually *differential* affinity between different subpopulations of neural crest cells.

Our foil barrier experiments also test the role of extrinsic guidance cues in shaping the r4 stream. Interestingly, barriers in the r3 paraxial mesoderm that do not even block the migratory pathway are still able to affect migratory behavior exhibited by the cells. Repulsive guidance cues in the r3 paraxial mesoderm have been shown to be dependent on r3 in a time-dependent manner (Golding et al., 2002). Tantalum barriers are impermeable and could impede the diffusion of cues from r3 into the paraxial mesoderm. With permeable barriers, the r3

paraxial mesoderm stays clear of neural crest cells, and a new stream is sculpted adjacent to the barrier. Our results show the clear presence of extrinsic environmental cues in shaping the shape of the migratory stream of neural crest cells. We conclude that multiple mechanisms, such as the intrinsic affinity of neural crest cells to follow each other and the presence of repulsive in the extrinsic environment, together shape the migration of cranial neural crest cells. Further studies will be needed to figure out the relative importance of intrinsic and extrinsic mechanisms.

In Chapter 3, we describe how we test the Eph/ephrin signaling pathway for involvement during cranial neural crest cell migration. Previous work has pointed to the role of Eph/ephrin signaling in mediating segregation of adjacent streams of migratory neural crest cells, likely through adhesion and repulsion (Helbling et al., 1998; Smith et al., 1997). We perturbed the levels of Eph/ephrin in migrating neural crest cells by electroporating constructs to drive the expression of full-length ephrin-A5; a constitutively-active, truncated, cytoplasmic portion of EphA4 (EphA4(int)); and a kinase-dead version of EphA4(int). To our surprise, ectopic ephrin-A5 did not cause mixing between neural crest cells migrating to branchial arches 3 and 4. Instead, ectopic ephrin-A5 specifically causes r6 neural crest cells to cease migration prematurely, without a defect in pathfinding.

Ectopic levels of EphA4 activity, on the other hand, cause the general population of cranial neural crest cells to migrate erratically—that is, the cells often display drastic pathfinding errors such as migrating back to the neural tube

instead of towards the branchial arch, migrating into the r3 repulsive zone, or mis-migrating around the otic vesicle. These pathfinding errors are accompanied by increased velocity and lower directionality. Neural crest cells with ectopic EphA4 expression seem lost compared with their wild-type counterparts. Our results suggest the Eph/ephrin signaling pathway does not merely mediate repulsion between adjacent streams of migrating neural crest cells. Instead, proper levels of Eph receptors and ephrin ligands are likely involved in regulating and/or maintaining the extent of migration in addition a role as a guidance cue for migration. Likewise, our studies suggest molecules other than the Eph/ephrin family members are involved in guiding cranial neural crest migration.

### ***Future Directions***

This thesis describes our efforts to understand how the cranial neural crest migration pattern is shaped. Many studies on cell migration focus on the migration of cells in vitro and/or in static studies. Our approach is to investigate the process of migration in vivo, to follow the process of migration in real-time, and to quantify the dynamic behavior of migratory cells as they navigate the complex environment of an intact embryo. We are able to probe the relative contribution of various mechanisms in patterning the migration of cranial neural crest cells, to test the role of specific signaling pathways during the process of migration, and to follow subsequent changes in migratory behavior.

Within the intact embryo, the migratory cranial neural crest cells likely encounter numerous factors, such as those from nearby placodes or endoderm.

Future studies should focus on the identification and possible involvement of other cell surface molecules, such as neuropilin or semaphorins, which have recently been shown to be crucial to the proper migration of trunk neural crest cells (Gammill et al., 2006). Other Eph/ephrin family members might also be interesting, including ephrin-b1, since knockouts display a cell-autonomous requirement for ephrin-b1 function within migratory neural crest cells (Davy et al., 2004).

Our results suggest that distinct mechanisms guide the cranial neural crest cells in each stream. The r4 stream is sandwiched between two crest-free zones as it migrates to BA2 (Figure 4.0C), whereas the neural crest cells in the r6 stream and from the first few somites first migrate together, and then segregate between BA3 and BA4 (Figure 4.0D). Possible future studies could focus dissecting the guidance cues involved in the migration of different subpopulations of cranial neural crest cells.

Further studies into the distribution of possible signaling molecules within the cell surface would also enhance our understanding of how guidance cues might translate into migratory behavior. Recent studies of *cis* interactions between co-expressed Ephs and ephrins have found that ephrin molecules are able to cause downstream signaling independent of Ephs (Marquardt et al., 2005) or to modulate Eph receptor signaling (Hornberger et. al. 1999, Carvalho et. al. 2006). Figuring out whether the Ephs/ephrins are distributed in discrete microdomains within the cell surface will be crucial in understanding how these signaling molecules might be functioning. Detailed FRET studies could clarify

how much direct interaction takes place at the cell surface. Our results point to the likelihood of multiple guidance cues in addition to Eph/ephrin family members. Figuring out the distribution and interactions of guidance molecules within the migratory neural crest cells will help us to fully understand how cranial neural crest cells interpret signaling from a repertoire of guidance cues.

Another area of study that would greatly enhance our understanding of migration is figuring out what comprises the migration machinery within a neural crest cell, and how that machinery changes as the cell migrates. Our studies highlight the intrinsic ability of the neural crest cells to persist in their migration despite the presence of physical barriers or molecular perturbations. It is unclear how this innate motility is modulated by guidance mechanisms to result in directed migration. It would be interesting to see how extrinsic guidance cues interact with the cellular machinery to drive dynamic cellular extensions and rapid migration. The use of fluorescently labeled actin or cytoskeletal proteins coupled with perturbation of candidate guidance cues could aid these studies.

Finally, many different mechanisms have been put forth to help explain cranial neural crest migration. Modeling of the cranial region could prove useful in figuring out how cell intrinsic mechanisms fit in with extrinsic cues. Though we did not conduct an exhaustive study of each mechanism, the data in this thesis suggest cranial neural crest cell migration likely involves a combination of the mechanisms. We now have substantial cell-tracking data that could be used to seed a virtual model. It would be interesting to see how individual cell migration parameters, such as velocity, directionality, or track length, might affect the

outcome, or pattern of migration, in models with varying geometries and values to represent extrinsic cues.

### **References**

- Carvalho, R. F., Beutler, M., Marler, K. J., Knoll, B., Becker-Barroso, E., Heintzmann, R., Ng, T. and Drescher, U.** (2006). Silencing of EphA3 through a cis interaction with ephrinA5. *Nat Neurosci* 9, 322-30.
- Davy, A., Aubin, J. and Soriano, P.** (2004). Ephrin-B1 forward and reverse signaling are required during mouse development. *Genes Dev* 18, 572-83.
- Gammill, L. S., Gonzalez, C., Gu, C. and Bronner-Fraser, M.** (2006). Guidance of trunk neural crest migration requires neuropilin 2/semaphorin 3F signaling. *Development* 133, 99-106.
- Hornberger, M. R., Dutting, D., Ciossek, T., Yamada, T., Handwerker, C., Lang, S., Weth, F., Huf, J., Wessel, R., Logan, C., Tanaka H., Drescher U.** (1999). Modulation of EphA receptor function by coexpressed ephrinA ligands on retinal ganglion cell axons. *Neuron* 22, 731-42.
- Helbling, P. M., Tran, C. T. and Brandli, A. W.** (1998). Requirement for EphA receptor signaling in the segregation of *Xenopus* third and fourth arch neural crest cells. *Mech Dev* 78, 63-79.
- Marquardt, T., Shirasaki, R., Ghosh, S., Andrews, S. E., Carter, N., Hunter, T. and Pfaff, S. L.** (2005). Coexpressed EphA receptors and ephrin-A ligands mediate opposing actions on growth cone navigation from distinct membrane domains. *Cell* 121, 127-39.

**Smith, A., Robinson, V., Patel, K. and Wilkinson, D. G.** (1997). The EphA4 and EphB1 receptor tyrosine kinases and ephrin-B2 ligand regulate targeted migration of branchial neural crest cells. *Curr Biol* **7**, 561-70.

*Figure 4.0: Distinct mechanisms guide neural crest migration at r4 and r6*

(A) Cranial neural crest cells (green) arise from all levels of the hindbrain and the first few somite levels. (B) As cells disperse from the hindbrain, they segregate into three discrete streams. (C) The r4 stream is shaped by two regions of repulsive cues (pink). (D) The r6 stream is formed by neural crest cells from r6, r7, and the first few somite levels. Neural crest cells that migrate to BA3 and BA4 are not kept segregated. Cells from r6 primarily migrate to BA3, with a minority migrating to BA4 (black arrows). Neural crest cells from r7 and the first few somites will migrate laterally to sort primarily to BA4. MB, midbrain. r2, rhombomere 2. BA2, branchial arch 2.

